Proceedings

Introduction

Ocean wave information relies on the collection of oceanographic and meteorological data, analysis and interpretation of the data, and dissemination of the resulting information products. These products can range from statistical tables and charts to bulletins and technical reports. Operational oceanography is distinct in that the science is focused on the development of information products that are used for decision making. Ocean wave conditions are a major constituent in any operational plan and are important to support safe maritime activities such as navigation, loading ships, fishing, recreation, mineral extraction, power generation, and military exercises. This workshop goes beyond consideration of descriptive wave products such as spectra from buoys, hindcasts from historical weather records, and forecasts from wave models. It provides the opportunity for participants to share their procedures for preparing and distributing wave information products; workshop attendees will discuss how their products are actually used to support decision making. Scientists, engineers, and managers have been invited to present ideas, research results, case studies, work in progress, and system demonstrations related to the use of wave buoys, models, and information to support operations. Discussions will highlight how wave information is used to make decisions such as the issuance of warnings to mariners, evacuation of coastal areas, routing of ships into favorable seaways, and efficient deployment of marine spill response equipment. This workshop provides a forum for operational oceanographers to stimulate discussion, provide new insights, and provide feedback for focused experiments.

Workshop papers and presentations can be accessed online at URL:

http://scholarworks.uno.edu/oceanwaves/2015.

Organizing Committee

Workshop Chairs:

Dr. Bhaskar Kura, P.E., Director of Maritime Environmental Resources and Information Center (MERIC), University of New Orleans (Co-Chair)
Mr. C. Reid Nichols, Marine Information Resources Corporation (Co-Chair)

Moderators:

Dr. Don Wright, Southeastern Universities Research Association, Session I

Mr. James D. Dykes, Naval Research Laboratory, Session II
Mr. Eric Gay, Marine Information Resources Corporation, Session III
Dr. Richard Price, PAE, Session IV

Rapporteurs:
Mr. Christopher Brown, Marine Information Resources Corporation

Workshop Objectives

Topics that were discussed included, but were not limited to:
- Wave measurements to support coastal construction.
- Numerical studies of waves, currents, and sediment transport.
- Sediment model applications with wave observations.
- Coastal wave buoys to save lives and protect property.
- Accessibility of wave information for scientists, engineers, and managers.

Methodology

Presentations, break-out groups, and guided discussions. *A Pre-Proceedings was made available prior to convening of the workshop.*

Target Participants

Oceanographers, engineers, scientists, Meteorological and Oceanographic (METOC) Services Officers, aerographer mates, marine science technicians, field supervisors and managers from academia, government, and industry.

Number of Participants
The number of participants was limited to 50. Attendees were able to register online at:

http://scholarworks.uno.edu/oceanwaves/2015/.

Contents

Opening Comments

SURA and the Science of Collaborative Research

Dr. Don Wright
Director of Coastal and Environmental Research
Southeastern Universities Research Association
1201 New York Avenue, NW, Suite 430
Washington, D.C. 20005

SURA facilitates multi-institutional collaborations, develops data and model standards and frameworks, enables comparisons of multiple models and provides HPC, data archiving and visualization support.

The Southeastern Universities Research Association (SURA) is a 501(c)(3) founded in 1980 to "collaborate on transformational research, education and training of next generation scientists and engineers" and development across disciplines. The original focus was to design, bid for, build and manage the Thomas Jefferson Accelerator Facility (JLab) **,** a nuclear physics research facility in Newport News, VA. Today, SURA's Research Programs and initiatives include Nuclear Physics (JLab), Information Technology, Coastal & Environmental Research, and Minority Outreach. The program of immediate relevance to this workshop is Coastal and Environmental Research.

The ongoing NOAA-funded, SURA-led ***Coastal and Ocean Modeling Testbed (COMT)*** has demonstrated significant success in facilitating a multi-institutional collaboration. The COMT has shown that accessible and discoverable observational data integrated with an advanced suite of open source community models can enable discovery and innovation of large-scale processes. The goal has been to accelerate the transition of scientific and technical advances from the coastal ocean modeling research community to improved operational services**.**

A new SURA-led initiative is focused on ***Understanding and Modeling Risk and Resilience in Complex Coastal Systems*****.** This initiative involves integration of the natural and social sciences to mitigate the nation's risk of loss of life and physical and economic damage from natural and manmade hazards. The overall goal is to integrate social and natural sciences to assist planning and risk assessment of coastal_communities threatened by both long-term and event-driven (e.g., by severe storms) inundation, land loss, water quality degradation and resulting economic declines in industries such as tourism, fisheries and shipping.

Wave-related COMT activities to date have focused largely on predictions of deep-water conditions and on wave-storm-surge coupling. However, the intensely non-linear transformations that take place in the shallow waters of the inner shelf and surf zone play critical roles in driving the processes of coastal erosion, sediment redistribution and inundation height. Included are wave dissipation by bed friction, energy transfer to soft cohesive inner shelf beds, wave induced sediment transport and related shallow water wave transformations that condition the nature of wave spectra and breakers within the surf zone. Future Testbed activities should encourage participation of the nearshore research community. SURA can facilitate multi-institutional collaborations, develop standards and frameworks, enable comparisons of multiple models and provide High Performance Computing, data archiving and visualization support.

References

Luetich, R.A., L.D. Wright, R. Signell, C. Friedrichs, M Friedrichs, J. Harding, K. Fennel, E. Howlett, S. Graves, E. Smith, G. Crane, and R. Baltes, 2013, Introduction to Special Section on the U.S. IOOS Coastal and Ocean Modeling Testbed, J. Geophys. Res. Oceans, 118, pp 1-10

SURA, Workshop entitled, "Understanding and Modeling Risk and Resilience in Complex Coastal Systems," October 29 & 30, 2014, Southeastern Universities Research Association, 1201 New York Ave. NW., Washington, DC.

Session I – Use of wave information in support of marine operations

Wave information from a variety of sources directly supports marine activities ranging from research and development in the coastal ocean to weather forecasting and search and rescue. Many marine operations are limited by waves. For example, surface and subsurface tasks may be at risk from unacceptable wave-induced motions and contribute to impacts, broaching, and capsize events. Historical data, imagery, observations, and model output have all been demonstrated to measurably improve marine weather forecasts and safety on the seas. The following papers describe uses of wave information.

Extended Abstracts

INTENTIONALLY BLANK

Evaluating Sediment Stability at Offshore Marine Hydrokinetic Energy Facilities

Craig Jones [1)*], Grace Chang [1)] and Jesse Roberts [2)]
[1)] Integral Consulting Inc., 200 Washington St. Suite 101, Santa Cruz, CA
[2)] Sandia National Laboratories, 1515 Eubank SE, Albuquerque, NM
[*]Corresponding author: cjones@integral-corp.com

1. Introduction

Development of offshore alternative energy production methods through the deployment of Marine Hydrokinetic (MHK) devices, e.g. wave energy convertors (WECs), in the United States continues at a rapid pace, with significant investment in recent years. Installation of any offshore MHK infrastructure at the seabed may affect coastal sediment dynamics. It is therefore necessary to evaluate the interrelationships between hydrodynamics and seabed dynamics and the effects of MHK foundations and cables on sediment transport. The ultimate goal of these evaluation methods is to quantitatively evaluate changes to the baseline seabed stability due to the installation of MHK farms in the water.

2. Methods

The objective of the present study is to evaluate and validate wave, current, and sediment transport models that may be used to estimate risk of sediment mobilization and transport. While the methodology and examples have been presented in a draft guidance document [1], the current work presents an overall strategy for model validation, specifically for a case study in the Santa Cruz Bight, Monterey Bay, CA, USA. Innovative techniques to quantify the risk of sediment mobility have been developed to support these investigations. Public domain numerical models are utilized to estimate the near-shore wave climate (SWAN: Simulating Waves Near-shore) and circulation and sediment transport (EFDC: Environmental Fluid Dynamics Code) regimes. The models were validated with field hydrodynamic data. Sediment size information was provided by the United States Geological Survey (USGS) usSEABED sediment database program. Near-bottom current- and wave-induced shear stresses were computed and used directly to derive a sediment mobilization risk relationship.

3. Results

Model simulation results from one applied wave and current scenario indicated that MHK foundations and structures may reduce the risk of sediment erosion in the area behind the structure by reducing wave activity behind the structures. The results suggest an array installed at the case study location may induce sediment deposition behind the structures. Deposition could result in the potential for habitat alteration, both in proximity to the array or further downstream near the shoreline. The far-field change in risk along the coast, however, does not show any widespread alteration.

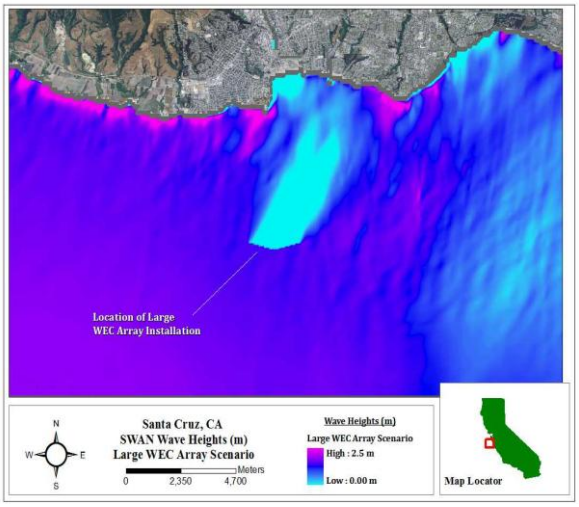

Figure 1. Case study model domain in the Santa Cruz Bight, Monterey Bay, CA USA.

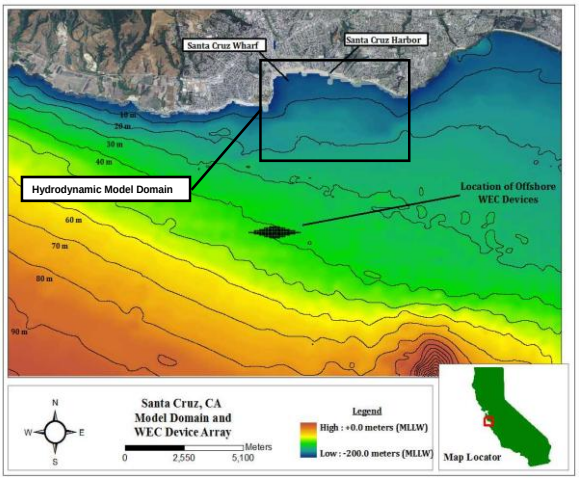

Figure 2. Simulated significant wave height in the presence of a WEC array.

4. Acknowledgment

This research was made possible by support from the U.S. Department of Energy's Wind and Water Power Technologies Office.

5. References

[1] Roberts, J. D., C. Jones, and J. Magalen. Offshore guidance document: Oceanography and sediment stability. SNL, Albuquerque, NM, 2013.

Session I Papers

INTENTIONALLY BLANK

Wave Energy Converter effects on wave, current, and sediment circulation: A coupled wave and hydrodynamic model of Santa Cruz, Monterey Bay, CA

Craig Jones [1)*], Grace Chang[1)], and Jesse Roberts [2)*]
[1)] Integral Consulting Inc., Santa Cruz, CA
[2)] Sandia National Laboratories, Albuquerque, NM
[*]Corresponding author: cjones@integral-corp.com

Introduction

Characterization of the physical environment and commensurate alteration of that environment due to Wave Energy Conversion (WEC) devices, or arrays of devices must be understood to make informed device-performance predictions, specifications of hydrodynamic loads, and environmental management decisions to physical responses (e.g., changes to circulation patterns, sediment dynamics). Wave energy converter devices will be deployed meters to several kilometers from the shoreline and are exposed to large forces from surface-wave action and currents which will define their performance. Wave-energy devices will be subject to additional corrosion, fouling, and wearing of moving parts caused by suspended sediments in the overlying water. The alteration of the circulation and sediment transport patterns may also alter local ecosystems through changes in benthic habitat, circulation patterns, or other environmental parameters.

The goal of this study is to develop tools to quantitatively characterize the environments where WEC devices may be installed and to assess effects to hydrodynamics and local sediment transport. The primary tools are wave, hydrodynamic, and sediment transport models. In order to ensure confidence in the resulting evaluation of system wide effects, the models are appropriately constrained and validated with measured data where available. Preliminarily, a model is developed and exercised for a location in Santa Cruz, CA for a hypothetical WEC array. An extension of the US EPA's (United States Environmental Protection Agency) EFDC (Environmental Fluid Dynamics Code), SNL-EFDC (Sandia National Laboratories EFDC) provides a suitable platform for modeling the necessary hydrodynamics and it has been modified to directly incorporate output from a Simulating WAves Nearshore (SWAN) wave model of the region. The modeling framework and results will be presented in this document.

Model Development and Application

Circulation and mixing in nearshore regions are controlled by nonlinear combinations of winds, tides, and waves. During a large wave event, wave effects can dominate the nearshore currents and mixing. The modeling approach for investigating WEC devices in the nearshore is structured to capture complex wave-induced currents and mixing, as well as tide- and wind-driven currents. This requires formulation and integration of both a wave model and a transport/circulation model. The final model results are ultimately linked to site-appropriate sediment properties to provide a full sediment transport model for investigating scour and suspended solids. The following sections outline the modeling components and application in Monterey Bay, CA.

Wave Model

The U.S. National Oceanic and Atmospheric Administration's (NOAA) operational wave model, WaveWatch III (NWW3), was used to generate deepwater wave conditions offshore of the site. WaveWatch III is a third-generation wave model developed at the NOAA National Centers for Environmental Prediction (NCEP). It has been extensively tested and validated. For oceanic scales and deep water, NWW3 has proven to be an accurate predictor of wave spectra and characteristics and has therefore become the operational model of choice for NCEP and many other institutions.

As deepwater waves approach the coast, they are transformed by processes including refraction (as they pass over changing bottom contours), diffraction (as they propagate around objects such as headlands), shoaling (as the depth decreases), energy dissipation (due to bottom friction), and ultimately, by breaking. The propagation of deepwater waves into each site was modeled using the open-source program SWAN, developed by Delft Hydraulics Laboratory, which has the capability of modeling all of these processes in shallow coastal waters.

Hydrodynamic Model

The hydrodynamic model used, SNL-EFDC, is based on a US-EPA-approved, state-of-the-art, three-dimensional hydrodynamic model developed at the Virginia Institute of Marine Science by John Hamrick [5], [6], & [7] to simulate hydrodynamics and water quality in rivers, lakes, estuaries, and

coastal regions. The SNL-EFDC includes improved hydrodynamics and sediment transport routines [8].

Bottom shear stress, τ_b, is produced at the sediment bed as a result of friction between moving water and a solid bottom boundary. The bottom shear stress is the fundamental force driving sediment transport. Shear stress is denoted as force per unit area (i.e., dynes/cm^2). It has been studied in detail for currents and waves, and can be defined and quantified mathematically given sufficient information about the hydrodynamics of the system. Shear stress is responsible for the initiation of sediment transport (i.e., erosion) and the ability of the flow to keep particles in suspension. The calculation of shear stress in areas such as the Santa Cruz region, where waves play a large role, is outlined in more detail by [2] and [3]. The wave- and current-generated bottom shear stresses are calculated in this effort using the [2] formulation.

The overall modeling approach has limitations that include:

- It is a simplification of a turbulent, chaotic, nearshore process.
- Salinity and temperature gradients are not included at the offshore boundaries. In other words, large-scale ocean circulation is not incorporated into the nearshore region.
- Measurements of currents are only available at nearshore locations for model validation.

Even though the above limitations are considered when assessing the results, this methodology produces accurate estimates of transport due to the dominant nearshore processes in the region (i.e., waves and tides). These can be used to develop quantitative relationships for sediment transport in the vicinity of marine hydrokinetic (MHK) devices and to assess the forces acting directly on the MHK devices.

Santa Cruz Wave Model

The Santa Cruz, CA, coastal region was chosen for the model framework development due to the similarity to the complex environments where MHK devices would be installed. In addition, under the US Department of Defense (DoD) Center for Excellence in Ocean Science (CEROS) research program, existing field data collection and model development efforts were leveraged for this task.

The NOAA operational wave model, NWW3, was used to generate deepwater wave conditions offshore of Monterey Bay, CA. Daily wave parameters, including significant wave height, peak wave period, and wave direction (H_s, T_s and D_p) were obtained for a reference point located at 37.00° N latitude, −122.5° W longitude. A SWAN model was nested with the NWW3 model to predict the propagation of waves into Monterey Bay and nearshore Santa Cruz, CA.

The Monterey Bay SWAN model domain is shown in Fig. 1. Both waves and wind were output at 3 hour time intervals from NWW3. This was the corresponding update duration for the Non-Stationary Monterey Bay SWAN model. NOAA National Data Buoy Center (NDBC) buoys within the domain are noted in Fig. 1. Data from NDBC Buoy 46236 were used to validate the model predictions for wave height, wave period, and mean wave direction. NDBC Buoys 46042 and 46091 were used to validate wind speed and direction. These buoys were selected based on the type of data that each recorded (i.e., Buoy 46236 did not record wind data, but recorded wave height and period). Buoy 46240 was located in shallow water near the southern Monterey Bay coastline, in an area not considered acceptable for deepwater model validation; therefore, its data were not used.

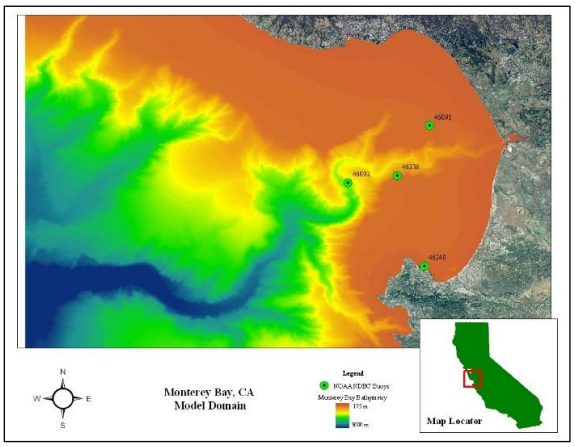

Figure 1. Monterey Bay model domain. NOAA NDBC buoys used for model validation are shown in green.

Wave conditions were outputted for a second nested model domain at a reference point 4 km south of Santa Cruz, CA. The coordinates of the output location were 36.9236° N, −122.0488° W. The grid resolution of the nested computational grid was approximately 0.0003° degrees in latitude and longitude (25 × 30 m^2 in x and y). The wave-spectrum boundary conditions were applied along the offshore (southerly) boundary of the Santa Cruz SWAN model domain. The model was run as a stationary model (no temporally varying wind-field updates). Winds were as-

sumed to have minimal effect on the nearshore wave conditions due to the relatively short distance from the offshore model domain boundary to the coastline. The Santa Cruz SWAN model wave conditions were updated during the period of study (10/18/2009 to 10/25/2009) with the daily Monterey Bay SWAN model output spectra.

A Datawell directional wave buoy (DWR-G) was deployed in the nearshore to measure wave heights, periods, and wave directions during the period of study. The buoy was deployed approximately 100 m south of the Santa Cruz Harbor shoreline and used to validate the nearshore model results. A Teledyne/RD Instruments Acoustic Doppler Current Profiler (ADCP) was deployed in proximity to the wave buoy. The ADCP measured current magnitude and direction in the water column.

Wave Model Validation

Wave heights (in meters), peak wave periods (in seconds), and mean wave direction (in degrees relative to True North) were obtained from the Monterey Bay SWAN model for validation with local NOAA NDBC buoys in Monterey Bay. Data were output every hour at several discrete buoy locations for direct comparison. The ability of a wind-wave model to predict wave characteristics can be evaluated in many ways. Here, model performance (model vs. measured) was assessed through the computation of a scatter index (SI), the root mean squared error (RMSE), and the bias, or mean error (ME). A scatter index [8] is defined as the RMSE normalized by the average observed value. Model performance was computed for both SWAN models: coarse grid Monterey Bay model and the nested, finer grid Santa Cruz model.

Wave heights, peak wave periods, mean wave directions, and total energy dissipation were output each hour from the Santa Cruz SWAN model for every grid point in the domain. The wave heights and wave periods were used to assess model performance with measurements from a locally deployed wave buoy. Output parameters (e.g. wave heights, radiation shear stresses, and dissipation) were used as input data to the nearshore SNL-EFDC model.

Fig. 2 is a comparison of model predictions and buoy measurements. The model performance statistics computed from the Santa Cruz SWAN model comparison to measured data also showed good agreement (see Table 1). The wave heights showed a mean error of +0.04 m (slight over prediction). All model performance values presented here are considered in good agreement. A more detailed description of the data collection effort and model validation conducted for the US Navy is outlined in [1].

Table 1: Model error statistics for the Santa Cruz SWAN model.

Data	RMSe	SI	ME
Hs	0.185	0.218	0.038
Tp	1.197	0.091	0.365
Dir	6.916	0.033	−1.53

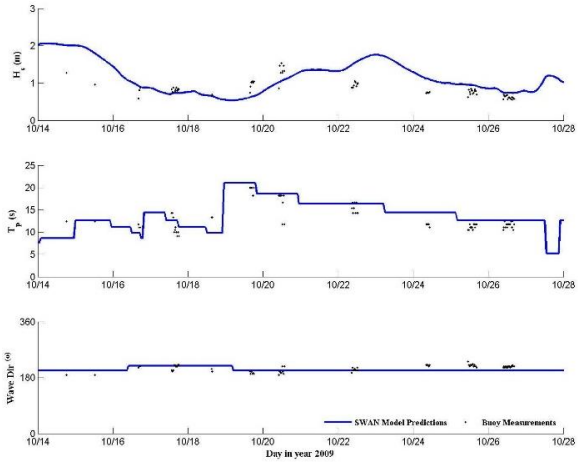

Figure 2. Model (line) representing the wave height (Hs), peak wave period (Tp) and mean wave direction (MWD) obtained from the Nearshore Santa Cruz SWAN model. Measured data (dots) were obtained from the Datawell DWR-G buoy deployed during the field study.

Santa Cruz Hydrodynamic Model

The initial development of the SNL-EFDC model required input of the regional coastal bathymetry. Bathymetry is represented in the numerical model through the creation of a grid and the specification of depth at each cell center. Grid dimensions are selected to balance desired resolution and computational cost. Grid cell size is 20×20 m^2, and the overall grid dimensions are 4.9 km in the alongshore direction (Point Santa Cruz to Soquel Point) and 3 km in the onshore-offshore direction.

The tidal water-level variations corresponding to the conditions in October 2009 were used as model boundary conditions. The water level was applied along the east boundary of the grid. The tidal water level variations were determined from the NOAA CO-OPS (Center for Operational Oceanographic Products & Services) values for tides in the Santa Cruz region (http://co-ops.nos.noaa.gov/index.html). Wind conditions over the model region were assumed

to be equivalent to the conditions measured at the Santa Cruz Municipal Wharf, which is central in the model domain. The hourly measured wind speed and direction from the wharf were applied over the entire model domain for the month of October 2009.

Hydrodynamic Model Validation

To ensure that the model accurately simulates currents in the project area, actual currents measured by a nearshore current meter deployed as part of the CEROS studies were compared with those simulated using the wave, tide, and wind boundary conditions outlined. The SWAN model was run for the entire field period to produce time series of wave parameters for the entire model domain. These results were incorporated into the SNL-EFDC model for the time period of interest with the actual tide and winds applied to the domain.

The peak wave heights on 10/14/2009 are shown in Fig 3. Figure 4 shows modeled shear stresses with velocity contours overlaid in the study area. These results demonstrate that along-shore velocities to the east are consistent with drifter observations and ADCP measurements made during the field measurement period. In addition, the combined wave and current shear stresses and velocities will provide the fundamental physical parameters for sediment transport studies under this task.

A quantitative comparison of measured data over the 4 days for which measurements were available to modeled nearshore, depth-averaged current magnitude data for the Santa Cruz nearshore currents model is presented in Fig. 5. Table 2 lists the model performance indicators. On average, the model under predicted the currents by less than 1 cm/s, which is within the 1.5 cm/s velocity error in the ADCP measurements. The combined wave and current model agreement with the measurements is considered excellent.

Table 2. Model error statistics for the Santa Cruz combined wave and current model.

Data	RMSE	SI	ME
Velocity	0.016	0.361	−0.008

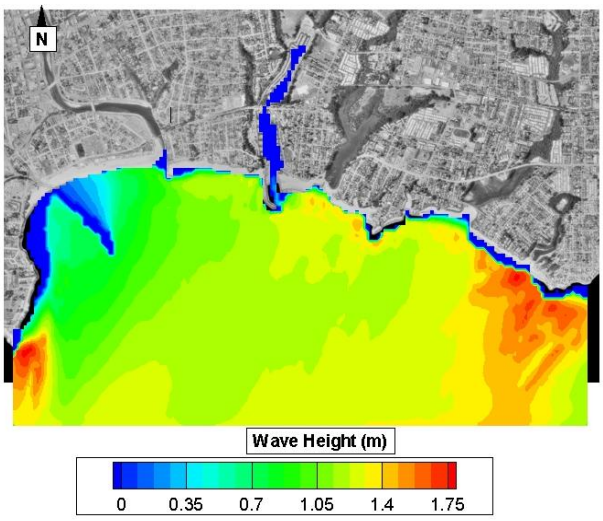

Figure 3. Peak wave heights in the model domain on 10/14/2009.

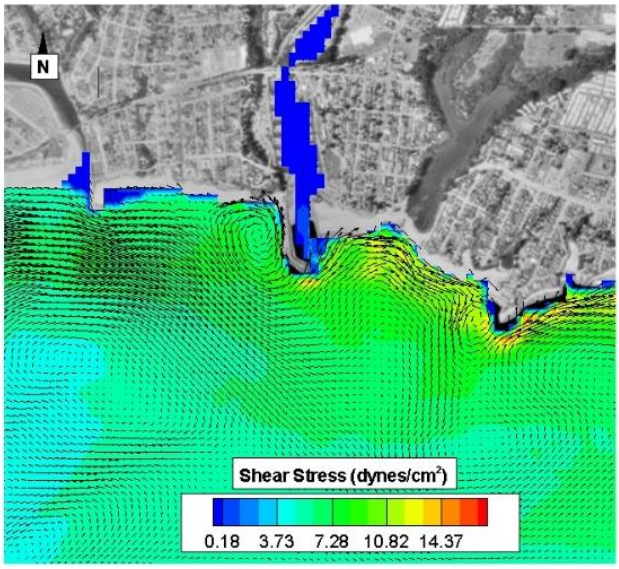

Figure 4. Combined wave and current shear stresses and velocity vectors in the model domain on 10/14/2009.

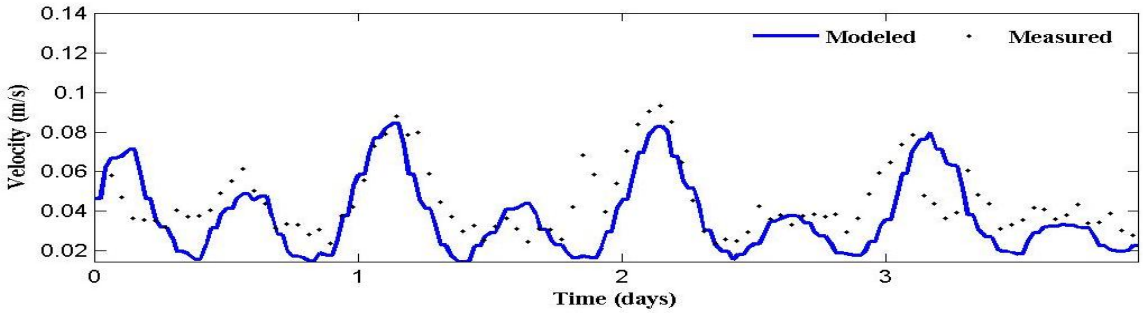

Figure 5. Model (line) representing the current magnitude obtained from the nearshore Santa Cruz SNL-EFDC model. Measured data (dots) were obtained from the RDI/Teledyne ADCP deployed during the field study.

Simulation of WEC Array

In this study, WEC devices are simulated in the SWAN model as discrete obstructions to the propagating wave energy and the subsequent wave fields are passed to the SNL-EFDC model as described above. For the investigation here, the modeled WEC array consisted of 200 individual point absorber style WEC devices organized into a honeycomb shape (Fig. 6). The center of the array was placed at the 40 meter depth contour. The WEC devices were modeled as 10 meter diameter structures spaced approximately 50 meters center-to-center. The distance between device edges was, therefore, approximately 40 meters (or 4 device diameters). The hydrodynamics and sediment transport domain, discussed in the following sections, is focused on the nearshore where the largest potential effects are anticipated. The area of this domain is highlighted in Fig. 6.

An environmentally conservative scenario was assumed for these simulations to evaluate the perceived largest potential effects of a WEC array on the local wave environment. Recent laboratory observations of wave propagation past a WEC array has indicated that "wave absorption is the dominant process inducing the wave shadow" [4]. As such, no wave energy was reflected from the WEC array within SWAN; while 100% of the wave energy was absorbed by the devices. This conservative absorption scenario created a wave shadowing effect in lee of the array. SNL is simultaneously performing related modifications to SWAN to more accurately represent WEC energy absorption that will be incorporated in upcoming work.

For these simulations two wave cases were investigated. A mean wave height of 1.7 m with a period of 12.5 was used as the average condition. Storm conditions were represented by the 95th percentile wave height of 3.5 m with a period of 17 s. The direction of the peak yearly wave energy is from the northwest. These cases are used as generally representative of average and extreme conditions. The modeled wave heights for the 1.7 m average wave case before and after WEC array installation are illustrated in Figure 7 and Fig.8. It is clear that inclusion of devices that inhibit wave propagation cause wave heights to be reduced behind the devices. The change in wave patterns as a result of the obstructions will be incorporated into the hydrodynamic model and subsequent sediment transport model.

Sediment Transport

Wave orbital velocities and wave-driven and tidal currents are among some of the predominant forcing mechanisms in near-shore regions. The combined forcing mechanisms cause shear stresses at the sediment-water interface. When the shear stresses are large enough, individual sediment particles will begin to mobilize, and may travel in bed load (along the seafloor) or become suspended in the water column and be transported with the ambient current. Waves are the primary source of shear stress at the sediment bed in the near-shore region that can cause resuspension of sediment; however, once suspended, sediments will be transported by the combined currents produced by waves and tides. Therefore, calculation of the combined wave-current interactions is necessary to truly represent the expected near-bed forces.

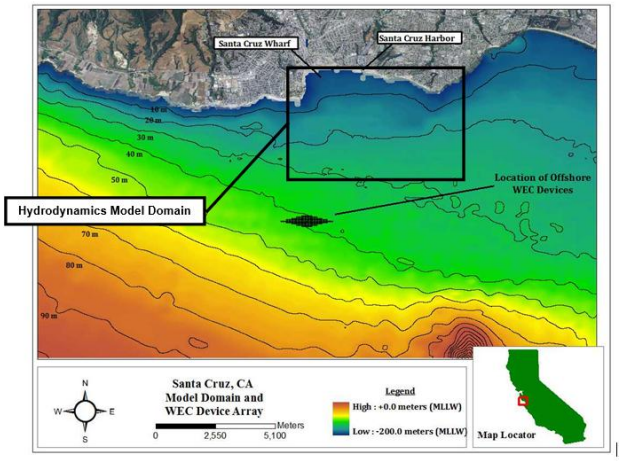

Figure 6. Near-shore Santa Cruz, CA, model bathymetry and WEC device array location.

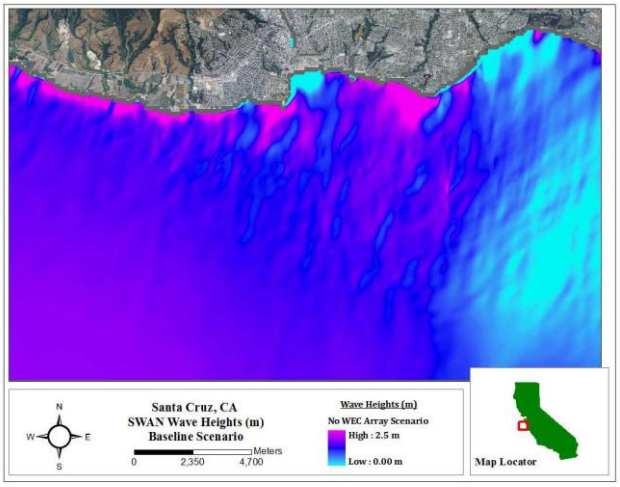

Figure 7. Modeled wave heights prior to the installation of a WEC device array.

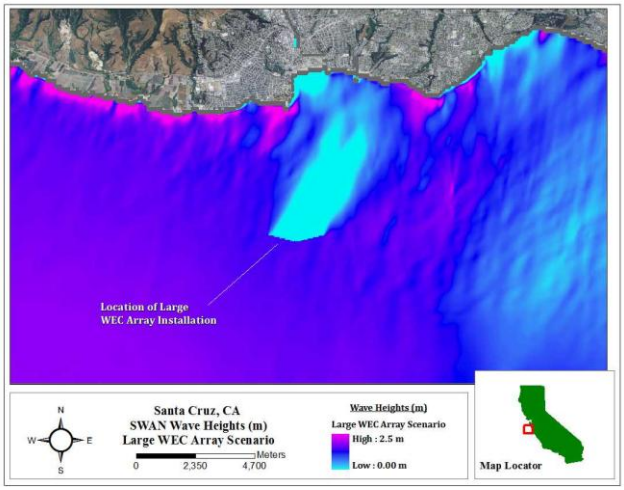

Figure 8. Modeled wave heights after the installation of a WEC device array for an incoming wave height of 1.7m.

.

The SNL-EFDC model was run for a one week period with the average and extreme SWAN wave characteristics incorporated (e.g. wave radiation stresses and energy dissipation). For the sediment transport simulations the average (1.7 m wave height) and extreme (3.5 m wave height) were used. Near-bottom shear stresses were computed due to the combined wave and currents from SNL-EFDC model following the method of [2], which accounts for the ambient current velocities, wave-induced orbital velocities and seabed roughness. The SNL-EFDC model takes account of multiple sediment size classes, has a unified treatment of suspended load and bedload, and describes bed armoring. Sampling efforts conducted by the USGS and Santa Cruz Port District were used to develop grain size maps of the model region. For these initial investigations a grain size distribution comprised of three separate size classes was developed from the data to define the initial sediment conditions. The size classes consisted of 200, 1000, and 3000 μm sediment representative of fine, medium, and coarse sand and the bed.

As an example of the nearshore changes in the sediment bed, changes after one month are examined. Fig. 9 shows a view of the circulation patterns and resultant bed change both before (baseline scenario) and after installation of the WEC array. Results are shown for the larger 3.5 m wave case.

The baseline results produce behavior consistent with observed nearshore circulation in the Santa Cruz region. The overall circulation and sediment transport are in a "downcoast" or easterly direction. The transport is divided into cells by the numerous rocky points in the region which are erosional (blue) while the beach regions retain sand (red). The blue streaks offshore are also observed in large scale multi-beam surveys of the area as transporting sand waves. The consistency of these results contributes to the overall reliability of the model.

Overall, the WEC array case shows less change in the sediment bed and a disruption of the common easterly currents developed in the nearshore region of Santa Cruz. The circulation in the lee of the array is also altered; reduction of energy in this region creates large offshore flow to balance the higher wave energy up and down the coast during the storm event. The disruption of circulation patterns can alter water quality and seasonal sediment transport patterns that must be investigated on a site specific basis. The implications of these results will be discussed further in the next section, however the comparison of the sediment bed height changes shows that there is a quantifiable effect on circulation patterns and sediment transport in the nearshore due to the presence of the offshore WEC array. It is generally evident that the WEC installation allows for more deposition, however there is a complex interplay that results in "hot spots" of sediment mobility.

Fig. 10 shows the difference in sediment bed height from the model for the 3.5 m storm wave height. The difference plot shows that generally the WEC installation allows for more deposition of any mobilized sediment, yet in the very nearshore to the east of the harbor excess sediment erosion can be seen. This is potentially due to the disruption of sediment supply to these areas during larger events which would normally inhibit erosion. The particle sizes decrease substantially offshore consistent with an overall reduction of wave energy and shear stress in the region allowing finer particles to accumulate at the surface. An unanticipated effect is the reduction of sediment deposition in the harbor mouth which could have a benefit of reducing dredging quantities required after large winter storms.

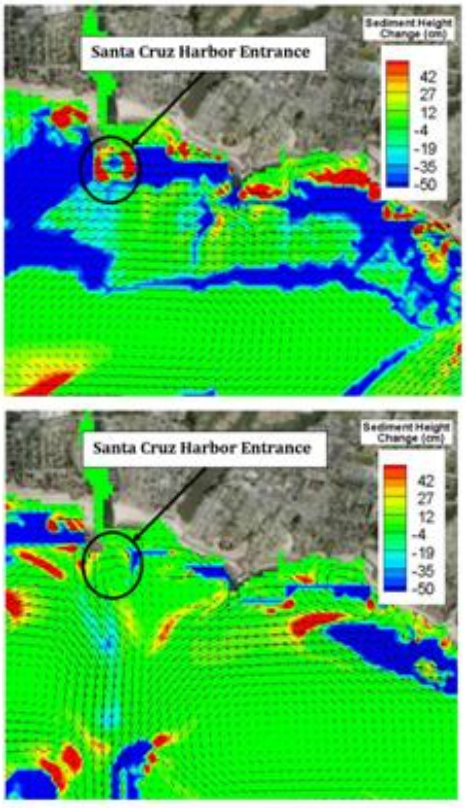

Figure 9. Velocity vectors and resultant sediment bed height change in cm from the combined wave and circulation model for the 3.5 m wave case. The top panel illustrates the baseline case and the lower panel shows the case with the offshore WEC array in place.

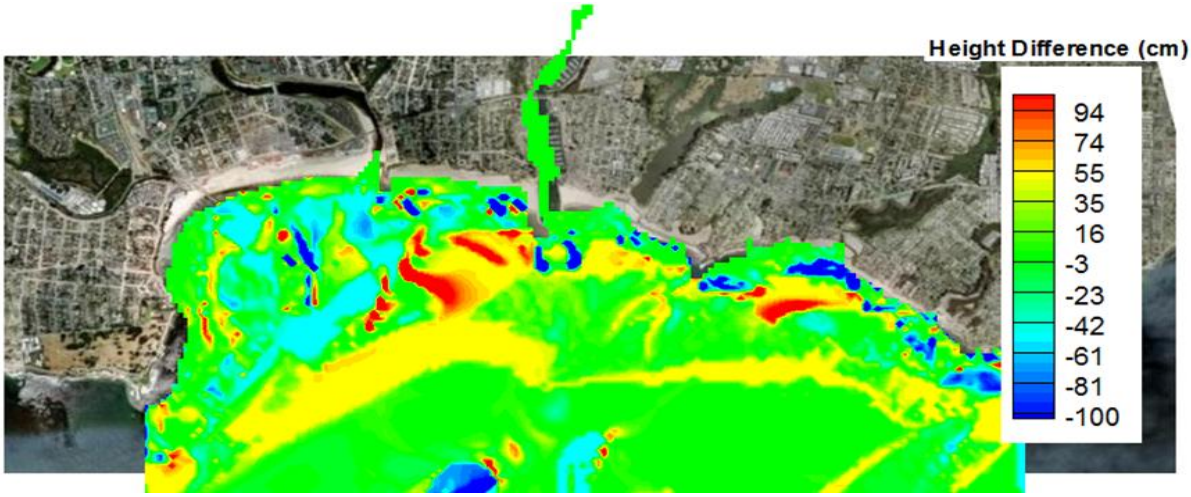

Figure 10. Comparison of change between the baseline model and the WEC array model from the combined wave and circulation model for the 3.5 m waves and normal tides.

Discussion

The goal of this study was to develop tools to quantitatively characterize the environments where WEC devices may be installed and to assess affects to hydrodynamics and local sediment transport. The SWAN wave model coupled with the SNL-EFDC hydrodynamic model developed for the Santa Cruz coast showed that the models accurately reproduced the wave heights and currents in the nearshore region. The large hypothetical WEC array investigated in the modeling study did show alterations to the wave and circulation properties. Differences in surface elevations between the two cases were used as a direct indicator of effects to the nearshore region. The results indicate that there is enhanced sediment trapping in the lee of the WEC array. The behavior is created by a low energy zone in the lee of the array bounded by large waves on either side. In general, the storm wave case waves and the average case waves showed the same qualitative patterns suggesting that these trends would be maintained throughout the year.

The modeling framework of SWAN and SNL-EFDC combined with field validation datasets allows for a robust quantitative description of the nearshore environment within which the MHK devices will be evaluated. This quantitative description can be directly incorporated into environmental impact assessments and eliminate the guesswork as to the effects of the presence of large scale arrays. It is important to emphasize that, in this analysis; all WEC devices are modeled using simple obstruction functions within SWAN that utilize *Transmission* and *Reflection* coefficients. In concurrent research activities, SNL has developed a modified version of SWAN, SNL-SWAN, to more accurately represent frequency dependent WEC power absorption and is presently comparing the model to experimental laboratory data. For the present study, an environmentally conservative approach (100% energy extraction) was used to represent WEC obstruction to wave propagation. This is considered environmentally conservative because physical environmental changes are expected to increase as more energy is removed from the propagating waves by WEC devices. In parallel activities, SNL is beginning to exercise SNL-SWAN within real-world model domains to more accurately characterize the alterations wave propagation and nearshore circulation and sediment transport.

References

[1] Chang, G., C. Jones, D. Hansen, M. Twardowski, and A. Barnard (2011) Prediction of optical variability in dynamic nearshore environments, Technical Report, SEI 11-01, Santa Cruz, CA, 530 pp.

[2] Cristoffersen, J., & Jonsson, I. (1985). Bed friction and dissipation in a combined current and wave motion. Ocean Engineering, 17(4), 479-494.

[3] Grant, W. D., & Madsen, O. S. (1979). Combined wave and current interaction with a rough bottom. Journal of Geophysical Research, 84(C4), 1797-1808.

[4] Haller, M. C., Porter, A., Lenee-Bluhm, P., Rhinefrank, K., and Hammagren, E. (2011). Laboratory Observations of Waves in the Vicinity of WEC-Arrays. Proceedings of the 9th European Wave and Tidal Energy Conference Series. Southampton, UK.

[5] Hamrick, J. M. (1992). A Three-Dimensional Environmental Fluid Dynamics Computer Code: Theoretical and Computational Aspects Virginia Institute of Marine Science (pp. 63): The College of William and Mary.

[6] Hamrick, J. M. (2007a). The Environmental Fluid Dynamics Code: Theory and Computation. In I. Tetra Tech (Ed.), (Vol. 1-3). Fairfax, VA: US EPA.

[7] Hamrick, J. M. (2007b). The Environmental Fluid Dynamics Code: User Manual. In I. Tetra Tech (Ed.). Fairfax, VA: US EPA.

[8] Komen, G. J., Cavaleri, L., Doneland, M., Hasselmann, K., Hasselman, S., & Janssen, P. A. E. M. (1994). scatter index (Komen et al. 1994. Cambridge, UK: Cambridge University Press.

Session I Presentation

The Session I Presentation can be accessed online at URL:

http://scholarworks.uno.edu/oceanwaves/2015/Session1/

Session I Notes

Use of wave information in support of marine operations

These notes are intended as a supplement to the presentation, "Wave Energy Converter effects on wave, current, and sediment circulation: A coupled wave and hydrodynamic model of Santa Cruz, Monterey Bay, CA." The following discussion points were captured by workshop rapporteurs:

- Wave energy converter (WEC) arrays have the potential to alter nearshore wave propagation, circulation, and sediment transport, all of which may have effects on ecological processes, shallow water processes, and socioeconomic services.

- Wave and hydrodynamics model simulations were used to quantify the potential effects of wave energy converter (WEC) arrays on nearshore wave propagation and circulation patterns in coastal Santa Cruz, CA. Results from the wave and hydrodynamics model were integrated with bathymetry and seabed characteristics to assess the risk of seabed stability alterations.

- The wave model, Simulating WAves Nearshore (SWAN), has been modified by Sandia National Laboratories (SNL) to account for the frequency and directionally dependent power absorption of WECs.

- Wave models and *in-situ* data can be used to create maps of seabed mobility risk (high versus low) for use by planners interested in siting structures such as wave energy converters.

- It is important to understand and validate a model's assumptions and boundary conditions with measurements.

- Different types of wave information are needed for a variety of users. While some operators require general wave information, others require statistics derived from long-term wave records.

- Key observations include significant wave height (m), dominant wave direction (degrees), wave period (s), 1D frequency spectral wave energy density (m^2/Hz) and 2D frequency-direction spectral wave energy density (m^2/Hz).

- Users may be interested in observations of sea, swell, wave steepness, surf and wave-induced nearshore currents.

- The observations of waves must be complemented by information on bathymetry and winds. Shallow water requires current bathymetry, which might be retrieved using imagery. High quality wind observations are essential for accurate Wavewatch III model forecasting.

- Buoy measurements and coastal radar systems provide valuable wave observations that meet user needs from mariners, wave enthusiasts, and city planners to coastal engineers and climatologists.

- Oceanographers and engineers rely on directional wave measurements to advance wave-modeling technologies.

- The real-time nature of wave information is particularly important owing to the response time of sea state parameters that are in sync with changes in wind speeds and directions.

- Archives of model input and output can be used for many applications including the assessment of sediment transport resulting from the installation of wave energy converters.

- Projects relevant to reference model development by Sandia National Laboratories in partnership with several national laboratories, academic institutions, and industry have data that could be archived in the NOAA Coastal and Ocean Model Testbed. The modeling effort in support of Wave Energy Conversion in Monterey Bay is applicable to other coasts.

- Wave data and information needs to be archived for subsequent use by researchers, especially those involved in resilience assessments. The archives need to use standard formats, especially to save information for extreme events such as tropical cyclones. Wave data from Hurricane Camille (1969), the second of three catastrophic Category 5 hurricanes to make landfall in the United States during the 20th century, are not readily available.

- Metadata is a crucial component of archived wave data.

- Funding agencies should require as part of any coastal project, the archival of wave data that are collected by project engineers and scientist. The archives should be made available for later use by community researchers.

Session II – Recent Developments in wave modeling with applications for operations

Ocean wave modeling services support a full range of maritime activities (e.g., shipping, fisheries, offshore mining, commerce, coastal engineering, construction, recreation, and scientific research). Innovations have related to the development of coupled ocean, atmosphere, wave, and sediment transport models. Many of these coupled models are focused on identifying significant processes affecting our coastlines and how those processes create coastal change. Applying wave modeling developments to marine operations ensures that research is practically focused. The following papers describe the use of wave models to support operations.

Extended Abstracts

INTENTIONALLY BLANK

Improving the Wave Forecasting in the Catalan Coast (WAM Cycle 4.5)

Adrià Moya[1,2)*], Agustín Sánchez-Arcilla[3,4)], Jesús Gómez[3,4)] and Gerbrant Ph. Van Vledder[2)]

[1)] Universitat Politècnica de Catalunya (UPC). Barcelona, Spain
[2)] Delft University of Technology, Civil Engineering and Geosciences Department, Delft, The Netherlands
[3)] Laboratori d'Enginyeria Marítima (LIM/UPC), Universitat Politècnica de Catalunya (UPC). Barcelona, Spain
[4)] Centre Internacional d'Investigació dels Recursos Costaners (CIIRC), Barcelona, Spain
[*]Corresponding author: adriamoyaortiz@gmail.com

Abstract

The present study investigates the conspicuous shortcomings of the whitecapping dissipation model implemented in WAM Cycle 4.5 [1], following the lead of the work of [2] and [3]. Its dependence on an overall wave steepness unavoidably yields systematic errors when more than one wave system is propagating.

The distinctive, complex orography of the Catalan littoral and the fact that the Mediterranean Sea is comparable to a semi-enclosed basin, brings about added difficulty when it comes to wave modeling. Additional reasons for the limited predictability include the shadow effect of waves due to the Balearic Islands, high wind variability in time and space, marked seasonality and relatively short periods associated with swell waves. These characteristics challenge the applicability of the current whitecapping formulation.

The main purpose of this study, therefore, is to investigate the effect of whitecapping dissipation on the temporal evolution of the wave spectrum, identify the causes that lead to significant errors and propose a suitable calibration of the tunable parameters of this least understood part of the physics, supported on comprehensive spectral and integral analyses. Such modifications attempt to correct, or at least improve, the frequent disagreement between predicted and observed wave data at the Catalan coast, especially during storm conditions. Particular attention is drawn to the Ebro delta area, not only because of the growing need to properly track its evolution but due to the common presence of characteristic bimodal spectra, caused by the coexistence of wind-seas and swells.

The WAM Cycle 4.5 [4] is run in two nested grids covering all the Northwestern Mediterranean Sea with a grid resolution from 9 to 3 km (Figure 10), forced with corresponding low and high-resolution six-hourly wind fields (WRF), for two typical storm events during January 2010. The results are validated at three different locations, where Directional Waverider buoys provide direct pitch-and-roll wave measurements. Identification of different wave systems is accomplished through reconstruction of buoys' two-dimensional spectra and further application of spectral partitioning techniques.

The aforesaid notwithstanding, results obtained from the tuning of parameters in the whitecapping dissipation function show a clear enhancement of the mean and peak wave periods for the study area, decreasing considerably the negative bias reportedly observed, whereas it is not possible to distinguish a representative improvement of wave heights by only tuning the whitecapping dissipation function. Even though new formulations seek for a more physical description of wave energy dissipation processes [5], [6], in the mean time, and for practical purposes, it is demanded a suitable set-up for the present model, in parallel with a full validation of upcoming source functions. As a final note, an improvement of wind field spatial and temporal resolution is required if aiming to capture local features such as coastal wind jets.

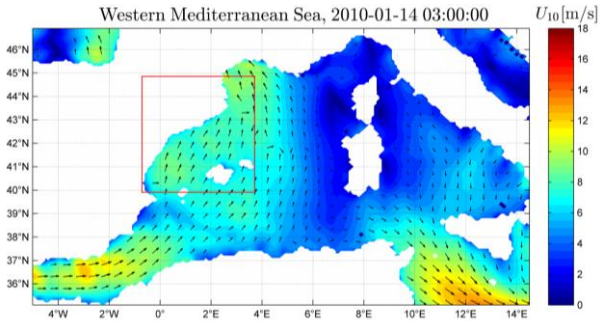

Figure 10. Northwestern Mediterranean grid (WM).

References

[1] G. J. Komen, S. Hasselmann, and K. Hasselmann, "On the Existence of a Fully Developed Wind-Sea Spectrum," *Journal of Physical Oceanography*, vol. 14, pp. 1271-1283, 1984.

[2] Elena Pallares, Agustín Sánchez-Arcilla, and Manuel Espino, "Wave energy balance in wave models (SWAN) for semi-enclosed domains-Application to Catalan coast," *Continental Shelf Research*, vol. 87, pp. 41-53, 2014.

[3] W. Erick Rogers, Paul A. Hwang, and David W. Wang, "Investigation of Wave Growth and Decay in the SWAN Model: Three Regional-Scale Applications," *Journal of Physical Oceanography*, vol. 33, 2003.

[4] WAMDIG, "The WAM model - A third generation ocean wave prediction model," *Journal of Physical Oceanography*, vol. 18, pp. 1775-1810, 1988.

[5] F. Ardhuin et al., "Semiempirical Dissipation Source Functions for Ocean Waves. Part I: Definition, Calibration, and Validation," *Journal of Physical Oceanography*, vol. 40, pp. 1917-1941, 2010.

[6] W. E. Rogers, A. V. Babanin, and D. W. Wang, "Observation-Consistent Input and Whitecapping Dissipation in a Model for Wind-Generated Surface Waves: Description and Simple Calculations," *Journal of Atmospheric and Oceanic Technology*, vol. 29, pp. 1329-1346, 2012.

Coastal and Ocean Modeling Testbed Applications

C. Reid Nichols [1)*], Robert G. Weisberg [2)] and André J. van der Westhuysen [3)]
[1)] Southeastern University Research Association, Washington, D.C.
[2)] University of South Florida
[3)] IMSG at NOAA/NWS/NCEP/Environmental Modeling Center, Maryland
[*]Corresponding author: rnichols@sura.org

1. Introduction

The Coastal and Ocean Modeling Testbed (COMT) was developed by the Southeastern Universities Research Association [1] under sponsorship from the National Oceanic and Atmospheric Administration (NOAA). The overarching goal involves establishing a testbed for verification of numerical models that improve the development of operational ocean products and the provision of marine services. The four pillars of COMT are (1) basic and applied research, (2) technology transition, (3) archival of discoverable information, and (4) dissemination of software tools.

2. Background

Numerous researchers, e.g., [2] and [3] working with COMT have applied wave (e.g., SWAN and *WAVEWATCH III*®) and circulation (e.g., ADCIRC, FVCOM, and SELFE) models to produce timely products characterizing extreme events that support decision makers. Archives that highlight wave heights and breaking waves during storms, storm surge during the passage of hurricanes, or river and coastal inlet plumes in synchronization with favorable winds are especially useful for contingency planning and coastal zone management. The COMT archive allows data innovators, who want to use model output to develop integrated products, to help operators anticipate the impacts of extreme events. COMT output can support exercises that help Commanders determine when to sortie Navy ships to avoid Hurricanes such as SANDY that occurred during 2012.

The archive includes input data, raw model output, as well as model output that has been quality controlled (removal of known errors) and/or "skill assessments" (addition of and comparison with observed data). This type of simulation information is invaluable for contingency planning (e.g., marine spill response, search and rescue, and use to support marine operations such as trans-ocean tows of large structures). Archived data have been produced using the oceanographic community's leading numerical models, whose outputs characterized important phenomena such as inundation, waves in a seaway, and sediment transport.

Data and information from the COMT collaboration website may be accessed from http://testbed.sura.org/datatable. As an example of data which could be used for severe weather planning are operational coastal surge and wave predictions and wave buoy data from Hurricane GEORGES, which made landfall on the SE of Puerto Rico (see Fig. 1). Significant surges were generated by GEORGES as the system moves over the reef shelf, strengthened by momentum transfer from wave breaking in shallow water [4].

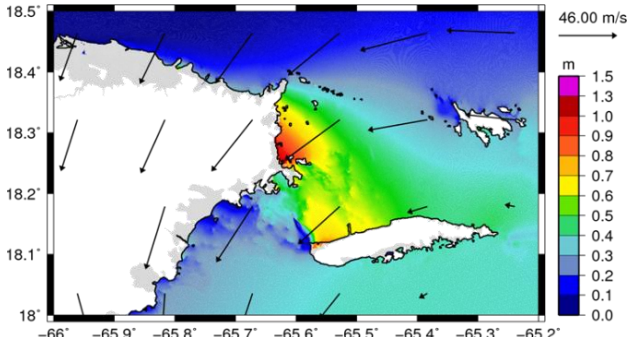

Figure 1. Model-derived coastal surge (m) during Hurricane GEORGES (1998) over the SE of Puerto Rico and the island of Vieques. Arrows indicate wind velocity vectors (obtained from [4]).

3. Applications

COMT supports organizations that need data and information to support hurricane evacuation planning, marine operations, safety, and environmental protection. Enhancements to the archive will be focused on development of simulations that support the Department of Homeland Security, especially in the development of baseline information that may support operational and contingency planning, training personnel to meet emergency response requirements, and providing authoritative environmental information to help operators carry out their missions successfully.

4. References

[1] Luettich, R.A., L.D. Wright, R. Signell, C. Friedrichs, M Friedrichs, J. Harding, K. Fennel, E. Howlett, S. Graves, E. Smith, G. Crane, and R. Baltes, 2013, Introduction to Special Section on the U.S. IOOS Coastal and Ocean Modeling Testbed, J. Geophys. Res. Oceans, 118, pp 1-10.

[2] Huang, Y., R. H. Weisberg, L. Zheng and M. Zijlema (2013), Gulf of Mexico hurricane wave simulations using SWAN: Bulk formula based drag coefficient sensitivity for Hurricane Ike. J. Geophys. Res., 2012JC008451, doi: 10.1002/jgrc.20283.

[3] Zheng, L, R.H. Weisberg, Y. Huang, R.A. Luettich, J.J. Westerink, P.C. Kerr, A. Donahue, G. Crane, and L. Akli (2013), Implications from Comparisons Two and Three Dimensional Model Simulations for the Storm Surge of Hurricane Ike. J. Geophys. Res., 2013JC008861, doi: 10.1002/jgrc.20248

[4] Andre J. van der Westhuysen et al. (2015). A Wave, Surge, and Inundation Modeling Testbed for Puerto Rico and the U.S. Virgin Islands: Year 1 progress. To be presented at the 95th AMS Annual Meeting, Phoenix, AZ.

Quantifying Wave Damping in *Spartina alterniflora*

Mary E. Anderson [1)*], Jane McKee Smith [1)]
[1)] Coastal and Hydraulics Laboratory, U.S. Army Engineer Research and Development Center, Vicksburg, MS
[*]Corresponding author: Mary.Anderson@usace.army.mil

1. Introduction

Coastal or tidal marshes serve as the interface between dry land and ocean waters throughout the world, and the ecological importance of these natural features is widely established. More recently, there is a growing interest in describing and quantifying the impacts of vegetation on coastal hydrodynamics. Although a body of literature investigating vegetation in unidirectional flows is relatively comprehensive, there is a paucity of research in comparison for oscillatory-dominated flows [1].

A parametric study investigating the dissipation of wave energy by artificial *Spartina alterniflora* was performed in a large-scale flume. *Spartina* is the dominant emergent seagrass of Atlantic Ocean and Gulf of Mexico tidal marshes. The study focused on irregular wave trains, with varied significant wave heights (5.0-19.2 cm), peak periods (1.25-2.25 s), water levels (2 submerged, one emergent), and stem densities (200 and 400 stems/m^2). Bulk trends in wave attenuation and changes in spectral shape are discussed. Implementation of vegetation dissipation into the nearshore spectral wave model STWAVE is validated using the original solution [2]. Following validation, STWAVE is applied to the laboratory measurements to explore the behavior of the bulk drag coefficient.

2. Methods

The physical model experiments were completed in a wave flume measuring 64.1 m long, 1.5 m wide, and 1.5 m deep at the U.S. Army Engineer Research and Development Center. The vegetation field started 1.2 m after the transition from the 1/20 slope to a flat bottom and measured 9.8 m long. Free surface oscillations were measured by 13 capacitance wave gauges sampling at 25 Hz.

Polyolefin tubing was selected to serve as the artificial *Spartina* as it fulfilled three basic requirements: simulate basic morphology of a plant stem, reproduce the swaying motion of seagrass under wave action, and remain upright in shallow water to model emergent conditions. The tubing was cut into equal lengths of 41.5 cm and had a diameter of 6.4 mm, which is similar to values reported for real *Spartina* [3].

3. Results and Discussion

An increase in stem density and submergence ratio (ratio of stem length to water depth) resulted in a significant increase in wave attenuation for all wave

Figure 1. Artificial *Spartina alterniflora* bed.

conditions. Larger wave heights increased wave attenuation slightly, and no clear trend with respect to wave period was found. Although energy dissipation was observed at all frequencies of the wave spectra, higher-frequency components were dissipated more efficiently. The attenuation of higher frequencies is addressed by characterizing the spectral tail as an exponent function of frequency and exploring deviations from $f^{-4} – f^{-5}$. STWAVE was able to replicate the wave evolution trend of the experiments well, with a goodness of fit coefficient R^2 exceeding 0.90 for all comparisons. An empirical relationship between the bulk drag coefficient and the Reynolds number is reported.

4. Acknowledgment

This work was funded under the Wave Dissipation by Vegetation for Coastal Protection Work Unit under the Flood and Coastal Systems R&D Program, Engineer Research and Development System, U.S Army Corps of Engineers. The program manager is Dr. Cary Talbot, and the Technical Director is Mr. William Curtis. Mr. William Henderson assisted with the laboratory measurements.

5. References

[1] Nepf, H. Flow and Transport in Regions with Aquatic Vegetation. Annual Review of Fluid Mechanics, 44: 123-142, 2012.
[2] Mendez, F.J. and I.J. Losada. An Empirical Model to Estimate the Propagation of Random Breaking and Nonbreaking Waves Over Vegetation Fields. Coastal Engineering, 51: 103-118, 2004.
[3] Feagin, R.A., J.L. Irish, I. Möller, A.M. Williams, R.J. Colón-Rivera, and M.E. Mousavi. Short Communication: Engineering Properties of Wetland Plants with Application to Wave Attenuation. Coastal Engineering, 58: 251-255, 2011.

Energetic Surface Waves Measured in Arctic Ice

Clarence O. Collins III [1)*], W. Erick Rogers [2)], Aleksey Marchenko[3)], and Alexander Babanin[4)]
[1)] ASEE Postdoctoral Fellow, Naval Research Laboratory, Stennis Space Center, MS, USA
[2)] Oceanography Division, Naval Research Laboratory, Stennis Space Center, MS, USA
[3)] The University Center in Svalbard, Longyearbyen, Norway
[4)] Swinburne University of Technology, Hawthorn, Australia
[*]Corresponding author: Tripphysicist@gmail.com

1. Introduction

The interaction between ocean surface gravity waves and sea ice in the Arctic Ocean is receiving renewed attention due to the rapidly changing Artic environment [1]. The role of waves in this environment is thought to become more important as reduced sea ice extent provides a greater Arctic fetch [2, 3]. Wave action may accelerate the retreat of ice by fracturing floes, which effectively enhances melting rates by increasing their surface area [1]. This feedback loop seems to be an important mechanism for understanding sea ice extent in Earth's future (i.e. warmer) climate [2]. As such, in situ measurements of waves in the Arctic are crucial for understanding these processes.

In addition, accurate prediction of sea state in ice covered areas of the oceans (and lakes) is important for safety during military and commercial sea going operations. To inform the representation of wave dynamics in ice covered regions [4], all possible sources of wave data are being explored [3]. Here we present an energetic wave event encountered by R/V Lance during a cruise just north of Hopen Island, off Svalbard, Norway on 2 May 2010.

2. Methods

The GPS records were corrected for time stamp errors and spikes and divided into hourly blocks for spectral analysis. The 3rd generation spectral wave model SWAN was applied following the path of R/V Lance. This particular wave model does not have a representation for ice, so model runs were interpreted as an "ice free" scenario. Since the dimensions of R/V Lance act as a low pass filter, only low frequency waves (less than 0.12 Hz) were considered for comparison. Bow-oriented, digital photographs were taken hourly during the cruise, providing a qualitative record of local sea ice conditions. For a larger scale picture of the sea ice extent, archived runs of the sea ice model PIPS were used.

3. Summary of Results

Three distinct phases of ice-wave interaction can be identified in Fig 1: 1) wave blocking by ice (red), 2) strong attenuation of wave energy and fracturing of ice by wave forcing (yellow), and 3) uninhibited propagation of the peak waves and an extension of allowed waves to higher frequencies (above the peak) (green), presumably due to interaction with ice floes which were made smaller by fracturing. The wave model severely over-predicts energy wave energy during phases 1 and 2 but accurately predicts the low frequency energy in phase 3. The propagation speed of the fractured-ice front is estimated to be of some fraction of the peak wave group velocity. The results--where the wave energy impacts the ice in a way that in turn affects the wave energy--imply that two-way, wave-ice coupling is necessary and the predictive skill of a wave model in an icy environment will depend critically upon the resolution and accuracy of the ice model. These are the largest waves recorded in the Arctic Ocean with substantial ice cover present and we expect large waves to occur more frequently as the sea ice extent lessens in the future.

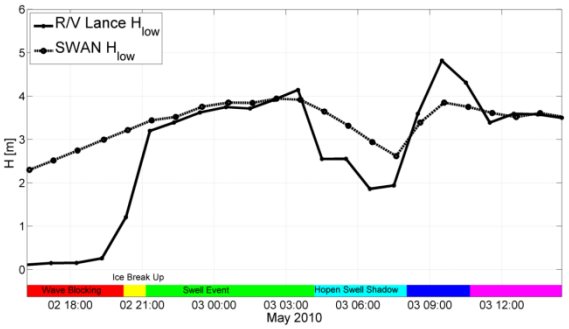

Figure 1. Low frequency wave height calculated from R/V Lance ship-borne GPS records and modeled with SWAN. Wave-ice interaction phases are color coded.

4. References

[1] Squire, V. (2007), Of ocean waves and sea-ice revisited, Cold Reg. Sci. Technol., 49(2), 110-133.
[2] Thomson, J. and W. E. Rogers (2014), Swell and sea in the emerging Arctic Ocean, Geophys. Res. Lett., 41(9), 3136-3140, doi:10.1002/2014GL059983.
[3] Asplin, M. G., R. Galley, D. G. Barber, and S. Prinsenberg (2012), Fracture of summer perennial sea ice by ocean swell as a result of Arctic storms, Journal of Geophysical Research: Oceans (1978–2012), 117(C6).
[4] Rogers, W. E. and M. D. Orzech (2013), Implementation and testing of ice and mud source functions in WAVEWATCH III®, NRL / MR / 7320-13-9462, 31 pp

Session II Papers

INTENTIONALLY BLANK

Improving the Wave Forecasting in the Catalan Coast (WAM Cycle 4.5)

Adrià Moya[1,2)*], Agustín Sánchez-Arcilla[3,4)], Jesús Gómez[3,4)] and Gerbrant Ph. Van Vledder[2)]
[1)] Universitat Politècnica de Catalunya (UPC). Barcelona, Spain
[2)] Delft University of Technology, Civil Engineering and Geosciences Department, Delft, The Netherlands
[3)] Laboratori d'Enginyeria Marítima (LIM/UPC), Universitat Politècnica de Catalunya (UPC). Barcelona, Spain
[4)] Centre Internacional d'Investigació dels Recursos Costaners (CIIRC), Barcelona, Spain
[*]Corresponding author: adriamoyaortiz@gmail.com

Abstract—The present study investigates the conspicuous shortcomings of the whitecapping dissipation model implemented in WAM Cycle 4.5 [1], following the lead of the work of [2] and [3]. Its dependence on an overall wave steepness unavoidably yields systematic errors when more than one wave system is propagating. The complex orography and highly variable winds at the Catalan coast lead to fetch- and duration-limited wave conditions near the Ebro delta. The incidence of swell trains during the development of these wind-seas coming from land favors the development of bimodal spectra. Although a comprehensive tuning of the free parameters of the dissipation function is performed, effectively improving the general subestimation of wave periods, it is strongly recommended to incorporate updated dissipation models, which avoid the dependence on an overall wave steepness and provide a more physical description of the wave breaking mechanism[4]; [5].

1. Introduction

This work was mainly originated with the goal of improving the current wave forecasting situation at the Catalan coast. It is known that the "Servei Meteorològic de Catalunya" (SMC), also known as "Meteocat", has driven its wave forecasts by using the wave model WAM over the Western Mediterranean Sea. Therefore, this study will be principally focused on getting deep insight into the wave model and, secondly, seeking the reasons by which non-negligible divergence exists between the outputs of such a model and the real measurements.

The main purpose of this study, therefore, is to investigate the effect of whitecapping dissipation on the temporal evolution of the wave spectrum, identify the causes that lead to significant errors and propose a suitable calibration of the tunable parameters of this least understood part of the physics, supported on comprehensive spectral and integral analyses. Such modifications attempt to correct, or at least improve, the frequent disagreement between predicted and observed wave data at the Catalan coast, especially during storm conditions. Particular attention is drawn to the Ebro delta area, not only because of the growing need to properly track its evolution but due to the common presence of characteristic bimodal spectra, caused by the coexistence of wind-seas and swells.

2. Physics

2.1. Energy balance equation

The evolution of the energy density $E(f,\theta)$ of each wave component can be obtained by integrating an energy balance equation while propagating with the group velocity along a wave ray:

$$\frac{\mathrm{d}E(f,\theta;x,y,t)}{\mathrm{d}t} = S(f,\theta;x,y,t) \quad (1)$$

where the term on the left-hand side is the rate of change of the energy density, and $\mathrm{d}x/\mathrm{d}t = c_{g,x}$ and $\mathrm{d}y/\mathrm{d}t = c_{g,y}$ (where $c_{g,x}$ and $c_{g,y}$ are the x- and y-components of the group velocity of the wave component under consideration), and frequency and direction are constant (in deep water). The term on the right-hand side (called the source term) represents all effects of generation, wave–wave interactions and dissipation. Developing the Eq. (1):

$$\frac{\partial E(f,\theta)}{\partial t} + \frac{\partial c_{g,x}E(f,\theta)}{\partial x} + \frac{\partial c_{g,y}E(f,\theta)}{\partial y} = S(f,\theta) \quad (2)$$

The source term $S_{tot} = S(f,\theta)$ is often written as:

$$S_{tot} = S_{in} + S_{nl4} + S_{ds} \quad (3)$$

These terms denote, respectively, wave growth by the wind, nonlinear transfer of wave energy through four-wave interactions and wave decay due to whitecapping wave breaking in deep water.

2.2. Source terms

The wind input formulation was adopted by [6] and the transfer of wind energy to the waves is described with a resonance mechanism [7] and a feed-back mechanism [8]:

$$S_{in} = \alpha + \beta E(f,\theta) \quad (4)$$

in which α describes the linear growth and $\beta E(f,\theta)$ exponential growth. For the WAM Cycle 4.5, although the model is driven by the wind speed at 10 m elevation U_{10}, it uses the friction velocity u_*. The computation of u_* is an integral part of the source term and it represents an alternative measure

for stress or momentum flux.

The second mechanism that affects wave growth in deep water is the transfer of energy among the waves, i.e., from one wave component to another, by resonance. The numerical implementation of the quadruplet wave-wave interactions is achieved with the development of the Discrete Interaction Approximation (DIA) as proposed by [9], which proved sufficiently economical for application in operational wave models.

Wave breaking in deep water (whitecapping) is a very complicated phenomenon, which so far has defied theoretical understanding. Generally, there is no accepted, precise definition of breaking and, additionally, quantitative observations are very difficult to carry out. Due to this reason, it is common practice to calibrate numerical wave models by tuning the parameters included in the corresponding formulation. In the present cycle of the WAM model, the process of whitecapping is represented by the pressure pulse-based model of [10], reformulated in terms of the wave number (rather than frequency), so as to be applicable in finite water depth (cf. [1]). This expression is:

$$S_{ds} = -C_{ds}\left[(1-\delta) + \delta\frac{k}{\langle k\rangle}\right]\left(\frac{\hat{s}}{\hat{s}_{PM}}\right)^{p}\frac{k}{\langle k\rangle}E(f,\theta) \qquad (5)$$

The coefficients C_{ds}, δ and p are tunable coefficients, $\hat{s}$ is the overall wave steepness, $\hat{s}_{PM}$ is the value of $\hat{s}$ for the Pierson- Moskowitz spectrum [11], and it is equal to $\hat{s}_{PM} = \sqrt{3.02 \times 10^{-3}}$. The values of the tunable coefficients in this model were obtained by [12] by closing the energy balance of the waves in idealized wave growth conditions (both for growing and fully developed wind-seas) for deep water. This implies that coefficients depend on the wind input formulation that is used. For the wind input of [13] and [14] it was obtained (assuming $p = 2$) $C_{ds} = 4.10 \times 10^{-5}$ and $\delta = 0.5$ (as used in the WAM Cycle 4; [14]). The theory on which the WAM model is based is described in more detail in [1].

3. The Catalan coast

The Mediterranean Sea is a semi-enclosed sea for it has limited exchange of water with the outer ocean. For practical reasons, it can be considered as a big lake in the sense that it is highly influenced by the coastline and the surrounding orography. Wave forecasting in this region is subject of extensive research and important progress has been achieved so far.

The reasons for the limited predictability in the study region are determined by a wave climate controlled by (1) short fetches, (2) shadow effect of waves from the south and east due to the Balearic islands, (3) complex bathymetry with deep canyons close to the coast, (4) high wind field variability in the time and space, (5) wave calms during the summer and energetic storms from October to May (marked seasonality), (6) presence of wind jets canalized by river valleys, (7) sea and swell waves combination that generate bimodal spectra and (8) relatively short periods associated with swell waves, which compromise the proper distinction between wind-sea and swell.

The abovementioned factors yield a characteristic behavior of integral parameters during storm conditions. More specifically, underestimation of wave height maximum values and overestimation of wave heights during calm periods is often observed [15]. Additionally, wave periods still suffer a notable underprediction. Pallares et al. [3], however, obtained a clear improvement of the mean wave period and the peak period at the Catalan coast, decreasing considerably the negative bias observed. Nevertheless, almost no change was observed in wave height due to the proposed modification.

Rogers et al. [2] observed a similar underprediction pattern and concluded that the cause lied in an underprediction of low- and medium-frequency energy in the modeled spectrum, together with an overly strong dissipation of the swell.

4. Model set-up

The WAM Cycle 4.5.3 [1] is run in two nested grids covering all the Northwestern Mediterranean Sea with a grid resolution from 9 to 3 km (Table 1), forced with corresponding low and high-resolution six-hourly wind fields (WRF), for two typical storm events during January 2010.

Table 1. Computational grids implemented in the wave model run for both Balearic (BS) and Western Mediterranean Sea (WM).

	Western Mediterranean Sea (WM)	**Balearic Sea (BS)**
Longitudes	4.95°W - 16.00°E	0.45°W - 5.58°E
Latitudes	35.10°N - 44.62°N	39.00°N - 43.66°N
Mesh size	196×119	168×173
Grid resolution	9 km (0.107°×0.081°)	3 km (0.036°×0.027°)

The frequency range considered is chosen according with the buoy frequency domain, which is 0.030–0.625 Hz, resulting in 33 frequency values that

range from 0.03 Hz to 0.633 Hz.

Additionally, the model runs are computed using a cold start. It has been observed, however, that the generation of wave forcing at the southern boundary of the coarse grid (WM), between the longitudes 10°E and 12°E, led no changes in the estimations at the three buoy stations. Note that this is only implemented at the very first step of the computation run; every new step assumes that the initial sea state is equal to the previous time step.

During the study interval (from Jan 6th to Jan 18th, 2010), waves were monitored by several wave-measuring instruments although the study presented herein uses three main buoys (Tortosa, Llobregat and Blanes; see Fig. 1). Directional Waverider buoys provide direct pitch-and-roll wave measurements. Identification of different wave systems is accomplished through reconstruction of buoys' two-dimensional spectra and further application of spectral partitioning techniques.

From this study interval, two storm events can be recognized based upon a reasonable threshold of 1.5 m of significant wave height (SWH) during more than 6 h [15]. The parameters considered for validation are:

SWH	H_{m0}	$H_{m0} = 4\sqrt{m_0}$
Mean-zero crossing period	T_{m02}	$T_{m02} = \sqrt{\frac{m_0}{m_2}}$
Peak period	T_p	$T_p = 1/f_p$
Mean wave direction	θ_m	$\theta_m = \tan^{-1}\left[\frac{\int \sin\theta\, E(f,\theta)\mathrm{d}f\mathrm{d}\theta}{\int \cos\theta\, E(f,\theta)\mathrm{d}f\mathrm{d}\theta}\right]$

5. Analysis of the results

5.1. First storm event (Jan 7th to Jan 12th, 2010)

This first storm is characterized by the dominance of two different sea states. First, wind coming from the east may correspond to air fluxes from the low pressure center over the sea. It is in this direction where developed wave conditions (associated with swell wave groups) may occur. On the other hand, wind coming from the northwest (at Tortosa) corresponds to air flow channeled by the Ebro river valley and blows towards the sea through the opening in the coastal mountain chain. The latter characteristic offshore-blowing winds result in fetch- and duration-limited growth conditions that commonly produce wind-sea waves at Tortosa.

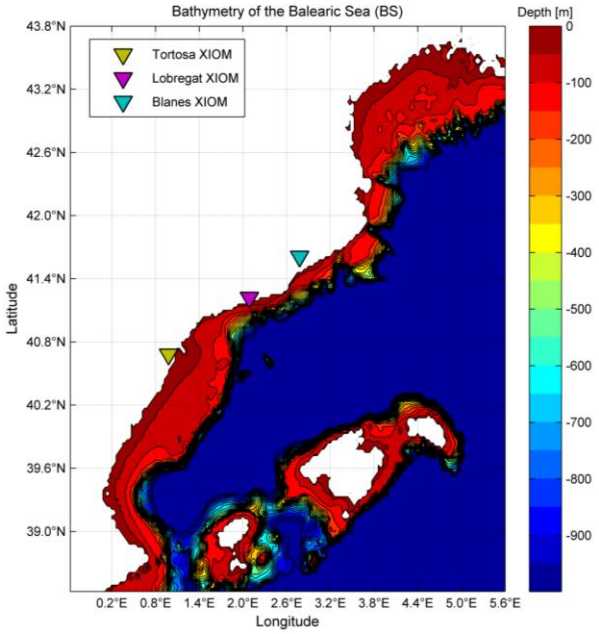

Figure 1. Bathymetry of the Balearic Sea (BS).

Swell waves are recorded during the peak of the storm (Jan 8th, at 00:00 h), whereas the second part of the storm, when swell dissipates, is determined by the mentioned wind-seas (see Fig. 2).

The energy content associated with the low-frequency peak is clearly underestimated regardless of the modifications proposed. Thereafter, it can be argued that there is an overly dissipation of energy by the time the storm reaches its peak (Jan 8th, at 00:00 h). Given the fact that wind-sea waves also grow during this first part of the storm, bimodal spectra are found at this location. The overall wave steepness, which largely affects the whitecapping dissipation model [Eq. (5)], increases, thus producing a higher energy dissipation rate. It can be seen, however, that the dissipation coefficient C'_{ds} significantly corrects this fictitious dissipation of low- frequency energy, when reduced to 0.5.

During the second part of the storm a better agreement is found. At this time, the energy spectrum widens and its peak shifts to higher frequencies due to the wind growth and progressive weakening of swell incidence. Here, a small dissipation coefficient yields too much energy (at all frequencies) and, hence, wave heights are slightly overestimated.

The mean wave period T_{m02}, on the other hand, is underestimated throughout the length of the storm (Fig. 3). It has been concluded that this is the result of

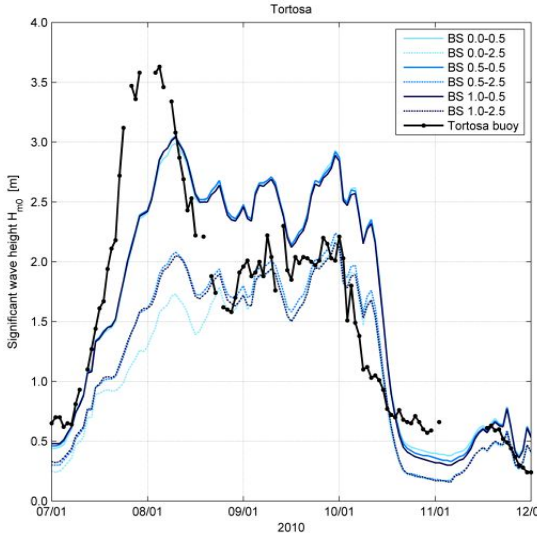

Figure 2. Comparison of temporal evolution of the significant wave height for different whitecapping coefficients at the buoy of Tortosa during the first storm event. Note that the combination of values stands for the delta and dissipation coefficient values ($\boldsymbol{\delta}$-$\boldsymbol{C'_{ds}}$).

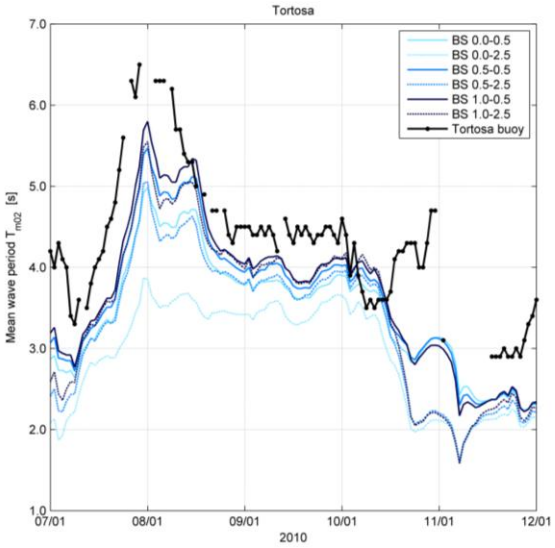

Figure 3. Comparison of temporal evolution of the mean (zero-crossing) wave period for different whitecapping coefficients at the buoy of Tortosa during the first storm event.

an overestimation of high-frequency energy in the wave spectrum. The physical description of the mean wave period is very sensitive to the amount of high-frequency energy due to the dependence on the second-order spectral moment m_{02}, which in turn is largely influenced by the square of the frequency. Therefore, the second-order spectral moment dramatically gives more weight to energy at high frequencies. Consequently, an overestimation of m_{02} leads to an underestimate of the mean wave period. Nevertheless, mean wave period can be substantially modulated and, most importantly, corrected by using a low dissipation coefficient and a large delta value ($\delta = 1$), thus enabling full dependence on the wave number [Eq.(5)].

Ultimately, mean wave directions are well reproduced by the model and only very small changes are induced by tuning the dissipation coefficients.

5.2. Second storm event (Jan 14th to Jan 16th, 2010)

The distinctive feature of the present storm event is the occurrence of a strong coastal wind jet off the coast at the Ebro delta. Even though presence of swell trains is reported during the beginning and end of such a storm, the most intense moments are driven by the high wind-energy input by part of the offshore-blowing wind associated with the coastal wind jet. In short, the main difference between this and the precedent storm is the sudden growth in wind speeds at Tortosa. Additionally, it can be seen that this strong wind event is locally generated and no large variations in wind velocity are reproduced in the two other

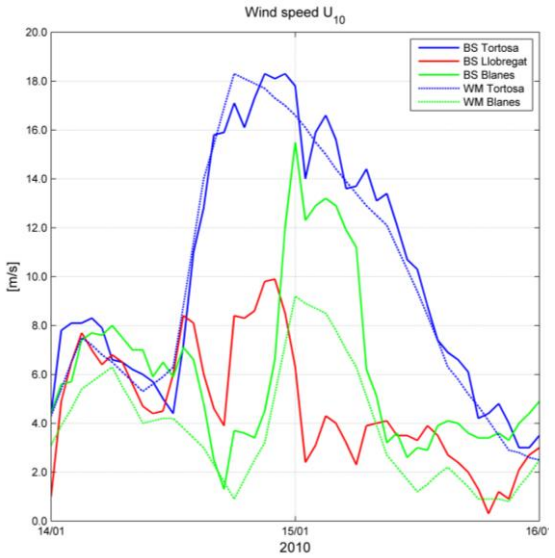

Figure 4. Temporal variation of computed wind velocities at the three different locations during the second storm event

locations (see Fig. 4), thus underscoring the consequential role played by orography.

Even though it could be stated that there is a general-

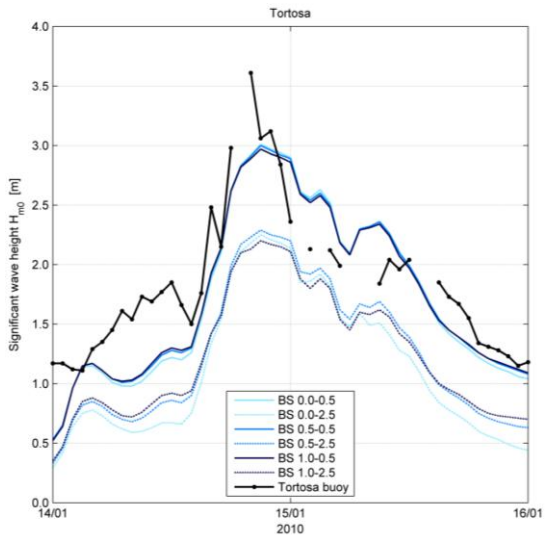

Figure 5. Comparison of temporal evolution of the significant wave height for different whitecapping coefficients at the buoy of Tortosa during the second storm event.

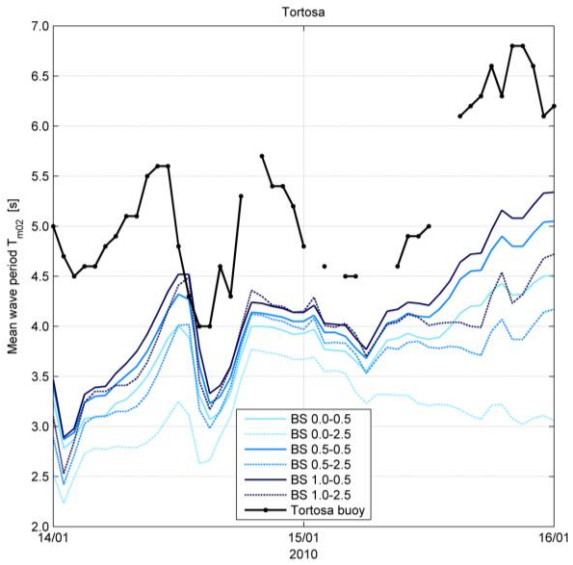

Figure 6. Comparison of temporal evolution of the mean (zero-crossing) wave period for different whitecapping coefficients at the buoy of Tortosa during the second storm event.

ized underprediction of wave periods and wave heights (not always true for the latter), better agreement between observed and estimated data exists in this second storm event. Despite the slight underestimation, significant wave heights are reasonably well predicted (for low-dissipation coefficients), although any of the proposed modifications captures the peak of the storm on Jan 14, at 21:00 h (see Fig. 5). The low-frequency energy (0.11-0.15 Hz), present during the first hours of the storm event, is clearly underpredicted, thus explaining the small wave heights at the beginning and agreeing with the fictitious dissipation of swell already found. Moving chronologically through the storm it can be seen that good agreement exists when it comes to low-dissipation coefficient combinations ($\boldsymbol{C'_{ds}} = \mathbf{0.5}$; the delta value hardly influences wave heights, in accordance with the previous storm).

The fact that an energy peak is generated right at the peak of the storm, over the whole frequency range, puts on record the high intensity and short duration of the coastal wind jet. However, given that it is not well-captured by the wave model, it suggests that this shortcoming lies in the fact that input wind fields have not correctly reproduced the sudden growth in speed.

The evolution of the mean and peak wave periods exposes the recurrent underprediction problem reported by many authors in semi-enclosed basins and bays. Therefore, both peak wave T_p and mean periods T_{m02} display differences of more than 1 s on average. However, in accordance with the analysis of the previous storm, the (1.0-0.5) combination provides best fitting (see Fig. 6). The existence of large scatter suggests that wave periods are strongly influenced by these two parameters (especially by the delta value, which balances the low- and high-frequency energy).

The last integral parameter reviewed is the mean wave direction (see Fig. 7), which is fairly well estimated; in particular wave groups coming from the south (Jan 14, between 00:00 and 15:00 h) and, later, associated with directions coming from the northwest (between the Jan 14, at 15:00 h and Jan 15, at 09:00 h).

6. Discussion

6.1. Impact on spectral energy

So far, underestimation of low-frequency energy has become a systematic error. Rogers et al. [2] suggested that underprediction of low-frequency energy can be attributed to one or more of the three deep-water source/sink terms and, focusing in the spectral dissipation, affirmed that can be also related to bulk parameters (e.g., mean steepness) that are influenced by the overly prediction of high-frequency energy.

Rogers et al. [2] reported successful results tuning the exponential coefficient $\boldsymbol{p}$ to 2 in the whitecap model [Eq. (5)], leading to an increase of energy at low fre-

quencies and decreasing high-frequency energy. This is due to the fact that the exponential coefficient acts on the wave steepness and, therefore, larger steepness associated with high-frequency waves will lead to larger dissipation, thus decreasing energy at that frequency range. In the present report it was not attempted to tune this third coefficient and, following the lead of [2], it was left by default at 2. A strong

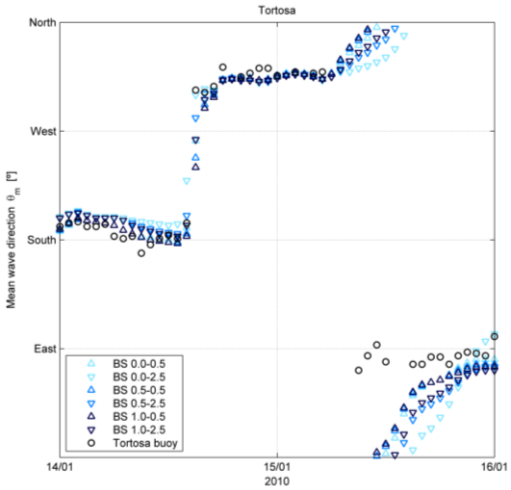

Figure 7. Comparison of temporal evolution of the mean wave direction for different whitecapping coefficients at the buoy of Tortosa during the second storm event.

focus has been placed, however, on tuning the two remaining parameters ($\boldsymbol{C'_{ds}}$ and $\boldsymbol{\delta}$).

The wave model (WAM Cy 4.5.3) dissipation source function was reformulated in terms of a mean wave steepness and a mean frequency in order to give more emphasis on the high-frequency part of the spectrum (based on [10]'s analytical model for whitecap dissipation according to [12]). Unfortunately, all tests by [12] were performed for wind-sea growth in the absence of swell, which was later found to generate problems inherent to the definition of a mean steepness from the entire spectrum, leading to overestimations of wind-sea growth in the presence of swell, even with the latest modification to [12]'s formulation by [16].

This shortcoming can be clearly seen during the low-frequency energy dominant peak generated at the beginning of the first storm event, in presence of a wind-energy input at higher frequencies or, similarly, when the wind-wave growth develops during the dissipation of the eastern swell in the same storm. Bimodality exists in both situations although a dominant wave group can be discerned in each one. Even though one might need to carefully examine it, low-frequency energy is always underestimated (below 0.10 Hz) and high-frequency energy is overestimated most of the time, especially when wind-sea energy is dominant (above 0.30 Hz). The latter overestimation might not be only induced due to low dissipation (resulting from mean wave steepness) but the approximation of the spectral tail, which seems to substantially yield too much energy at high frequencies.

6.2. Impact on integral parameters

Different impact on integral parameters is driven by each coefficient. Significant wave heights are largely influenced by the dissipation coefficient C'_{ds}, which in turn has lower effect on wave periods. This is due to the fact that whitecapping dissipation has linear dependence on this coefficient [Eq.(5)] and, therefore, if reduced, lower dissipation is guaranteed for the whole frequency range, leading to a larger overall amount of spectral energy and, hence, larger wave heights. The delta value, on the other hand, modulates the dependency on the wave number (i.e., the length of the waves) and its contribution is more subtle.

When the delta coefficient is raised to 1, maximum dependence on wave number is assured, thus yielding more dissipation at high-frequencies (short wave lengths) and lower at low-frequencies (long wave lengths). Due to the latter statement, better agreement is provided when delta is raised, thus coping with the negative adverse effect introduced by the dependence on the mean wave steepness. In addition, when implementing this modification, whitecapping dissipation places more weight on the high-frequency range and, as a result, the second-order spectral moment reduces because of the lower energy content at high frequencies. This outcome results in a substantial enhancement in the mean wave period T_{m02}, thus improving the well-known tendency to underpredict this parameter in the Catalan coast.

6.3. Statistical analysis

Even though statistical parameters are representative when long time series are available (two or three months, at least), they give a quantitative evaluation of the degree of accuracy of simulation results and will serve to support the results of the spectral analysis. The main statistical parameters are the root mean square error (RMSE), the bias, the scatter index (SI), the correlation coefficient (R) and the mean absolute error (MAE):

$$\text{RMSE} = \sqrt{\frac{1}{N}\sum_{i=1}^{n}(S_i - O_i)^2} \qquad (6)$$

Table 2. Summary of the statistical errors for the simulations during the first storm event.

	RMSE			**BIAS**			**SI**			**R**			**MAE**	
	WM	**BS**		**WM**	**BS**		**WM**	**BS**		**WM**	**BS**		**WM**	**BS**
1.0-0.5														
H_{m0}	**0.531 m**	**0.580 m**		-0.071 m	**0.162 m**		**0.337**	**0.368**		**0.805**	**0.811**			
T_p	2.465 s	**2.271 s**		**-1.201 s**	**-0.962 s**		0.369	**0.340**		0.471	**0.520**			
T_{m02}	**0.954 s**	**0.760 s**		**-0.790 s**	**-0.588 s**		**0.221**	**0.176**		0.776	**0.829**			
θ_m	100.756°	92.150°		26.151°	13.232°		0.501	**0.458**		0.666	**0.710**		43.565°	38.323°

Table 3. Summary of the statistical errors for the simulations during the second storm event.

	RMSE			**BIAS**			**SI**			**R**			**MAE**	
	WM	**BS**		**WM**	**BS**		**WM**	**BS**		**WM**	**BS**		**WM**	**BS**
1.0-0.5														
H_{m0}	**0.418 m**	**0.359 m**		-0.251 m	0.180 m		0.229	**0.196**		0.898	0.883			
T_p	**1.713 s**	**1.721 s**		**-1.261 s**	**-1.259 s**		**0.229**	**0.230**		**0.808**	**0.808**			
T_{m02}	**1.300 s**	1.196 s		**-0.790 s**	**-1.098 s**		**0.248**	**0.228**		**0.783**	**0.791**			
θ_m	75.337°	64.260°		15.414°	2.756°		0.399	0.340		0.725	0.784		17.951°	17.146°

$$\text{bias} = \frac{1}{N}\sum_{i=1}^{n}(S_i - O_i) \quad (7)$$

$$\text{SI} = \frac{RMSE}{{}^{1}/_{N}\sum_{i=1}^{n} O_i} \quad (8)$$

$$\text{R} = \frac{\sum_{i=1}^{n}\{(S_i - \langle S\rangle)(O_i - \langle O\rangle)\}}{\sqrt{\{\sum_{i=1}^{n}(S_i - \langle S\rangle)^2\}\{\sum_{i=1}^{n}(O_i - \langle O\rangle)^2\}}} \quad (9)$$

$$\text{MAE} = \frac{\sum_{i=1}^{n}\Delta\theta_{O,S}}{N} \quad (10)$$

where O_i is the observed value, $\langle O\rangle$ is the mean value of the observed data, S_i is the simulated value, $\langle S\rangle$is the mean value of the simulated data and N is the number of data. The shortest distance $\Delta\theta_{1,2}$ between two directions is computed as: $\Delta\theta_{1,2} = 180 - \left|180 - |\theta_1 - \theta_2|\right|$.

Table 2 and Table 3 display the above mentioned statistical parameters for the chosen combination (1-0.5) of whitecapping coefficients and integral parameters.

Significant wave heights show higher correlation in general, although there is no clear trend with respect to positive or negative bias. This, however, is completely true for wave periods. Negative bias in both mean and peak wave periods is observed in both storm events, regardless of the combination proposed. A result of value is displayed by the very low correlation coefficient exhibited by the peak period during the first storm (characterized by bimodal spectrum). Similar bias is found in peak periods during both storms; however, in the first event larger scatter and root mean square errors are displayed. Another outcome that agrees with visual analysis is the fact that larger errors are encountered in mean wave directions during the first storm, in which different wave systems are found propagating in different directions at the same time.

It is also of interest to compare the results computed at different scales (i.e., different computational grids). Better agreement is found in virtually every parameter belonging to the high-resolution domain (BS), in relation with the coarse domain (WM). It is perhaps more interesting to note that some parameters provide better results when using data coming from the coarse grid (e.g., the scatter index SI for wave heights during the first storm; not shown here). Scatter indexes are expected to be lower with high-resolution data due to the enhanced accuracy (see Fig. 8).

Bertotti and Cavaleri [17] obtained systematically higher scatter in their small scale model and suggested that although ironically, this fact represents the capability of the high-resolution simulations (small scale) to go into higher details of the fields. However, the capability of reproducing realistic details does not imply these details are correct. Given a certain level of scatter between the actual data and a relatively smooth (lower resolution) field, the introduction of higher resolution details, physically consistent but not necessarily coincident with the real ones, leads una-

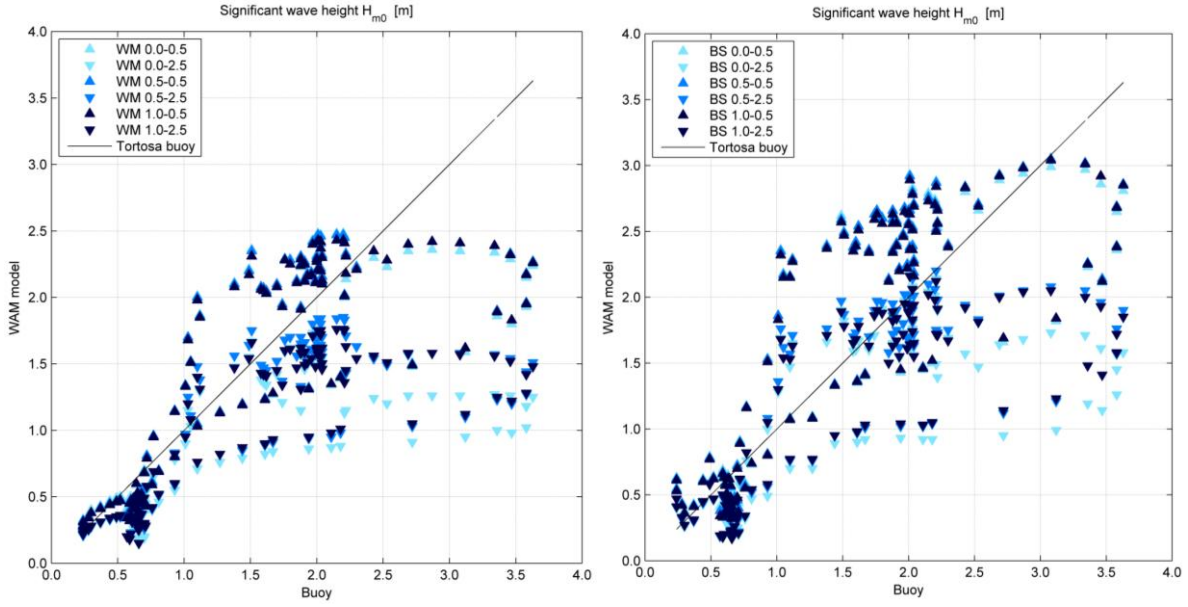

(a) Large-scale simulation (WM) (b) Small-scale simulation (BS)

Figure 8. Scatter plots for H_{m0} showing the larger scatter of the high-resolution simulation (BS). Results for the first storm event at Tortosa buoy.

voidably to a larger scatter (commonly referred as "double penalty").

Therefore, nested models, although capable of exceptional performances, cannot overcome all deficiencies. They simply focus on the details of a given area and, relying on their upper domain, do it correctly when correct information is provided [17].

6.4. Temporal and spatial resolution of wind fields

Furthermore, although not thoroughly explored in this research, it has been seen that the lack of temporal resolution in the wind fields can lead to not only underestimation, but even omission of the peaks and troughs of the temporal variations of significant wave height and average wave period. As an example, the large underestimation of the wind-sea peak (0.14-0.15 Hz) associated to the peak of the second storm (Jan 14, at 21:00 h): observed data suggest the existence of a coastal wind jet, the time scale of which was shorter than 6 h; thus pinpointing the too coarse temporal resolution of the wind fields implemented (6 h). Consequently, an increase of the temporal resolution is strongly recommended to properly capture the instantaneous effects of coastal wind jets at the buoy of Tortosa. On the other hand, it can be seen that the spatial resolution of the wind field is not as influential as the temporal at Tortosa. This can be concluded due to the fact that wind speed and directions are fairly similar in both fine (BS) and coarse (WM) grids (Fig. 4). However, in the same figure, important disagreement is found for the buoy of Blanes (and it is suspected that it would similarly occur at Llobregat). Alomar [18] reported the benefits of increasing wind variability in wave forecasting by increasing both the temporal and spatial resolution of the forcing wind fields. High resolution input winds prevent information losses in short-duration storm, especially in basins where the orography plays a substantial role.

7. Conclusions

The present (whitecapping) dissipation model [12] produces inconsistent results, especially marked differences with observed data during storm events. Although one cannot forget the important role played by the wind and nonlinear wave-wave interaction functions, it should be noted that dissipation of energy largely influences the energy balance and, hence, derived spectral parameters.

It has been found a low-frequency energy underestimation and high-frequency energy overestimation in the wave spectrum. This outcome was confirmed due to the overall steepness dependence of the dissipation model of [12]. The numerical implementation of the diagnostic tail might enhance this undesired effect. As a result, due to the different distribution of energy density, spectral moments will unavoidably change and, hence, spectral parameters such as H_{m0}, T_{m02} or T_p, will change as well. Therefore, an underestimation of wave periods occurs due to the over esti-

mation of high-frequency energy, whereas wave heights show no clear trend.

A low dissipation coefficient (C'_{ds}) and a delta value equal to 1 [Eq. (5)] yield a better agreement with observations. The fully dependence on wave number provided by this delta value compensates the spectral energy distribution explained in the second point, thus leading to slightly more energy at low frequencies and reducing the content at high frequencies [2], [3].

Evolution of coastal wind jets (as a result of the complex orography of the littoral) occurs at relatively short time scales (less than 6 h). Some observed peaks (e.g., H_{m0}) are missing in simulations. This is due to the fact that the time interval between consecutive wind fields is too large (6 h) and, therefore, wind-induced features occurring at time scales shorter than 6 h are not captured and reproduced by the model.

Nesting a computational grid (similarly for winds' mesh) with higher spatial resolution brings about more detailed results, which in most of the cases leads to better agreement with observed parameters.

8. Recommendations

Although it is argued that the present whitecapping formulation [12] produces inconsistent rates of energy dissipation, more satisfactory results (in storm conditions) can be obtained by keeping a low value for the dissipation coefficient, C'_{ds}, and setting the delta value, δ, equal to 1 (with the remaining tunable coefficient p equal to 2; [2].

Implement newer formulation for the dissipation source term [19] Recent formulation proposed by [4] and [5] offer better prospects for progress, although not fully tested. Therefore, for practical purposes, since WAVEWATCH III already incorporates [19]'s dissipation model, validation tests could be performed in order to evaluate the implementation of an updated formulation.

Prior to a calibration of wave growth rates and implementation of new source functions (if performed in future work), wind fields should be completely validated. Large sources of error generally come from wind fields rather than a not suitable description of the source terms.

Replacement of current six-hourly wind fields, by higher temporal resolution winds (at least three-hourly) in order to capture local features, such as the typical coastal wind jets, observed at the Ebro delta.

9. Acknowledgement

I would like to heartily thank Prof. Agustín Sánchez-Arcilla, who offered assistance and encouraged me to take on this research. Jesús Gómez, who I would like to express my sincere gratitude for his role in obtaining experimental data and proposing technical solutions. I owe special gratitude to Dr. Gerbrant Ph. van Vledder, who has provided me precious suggestions and advice. Without his guidance and encouragement through the past year at TUDelft, this study would not have been possible to accomplish. My sincere thanks also go to Elena Pallarès, who has provided me with constructive suggestions.

10. References

[1] WAMDIG, "The WAM model - A third generation ocean wave prediction model," *Journal of Physical Oceanography*, vol. 18, pp. 1775-1810, 1988.

[2] W. Erick Rogers, Paul A. Hwang, and David W. Wang, "Investigation of Wave Growth and Decay in the SWAN Model: Three Regional-Scale Applications," *Journal of Physical Oceanography*, vol. 33, 2003.

[3] Elena Pallares, Agustín Sánchez-Arcilla, and Manuel Espino, "Wave energy balance in wave models (SWAN) for semi-enclosed domains-Application to Catalan coast," *Continental Shelf Research*, vol. 87, pp. 41-53, 2014.

[4] F. Ardhuin et al., "Semiempirical Dissipation Source Functions for Ocean Waves. Part I: Definition, Calibration, and Validation," *Journal of Physical Oceanography*, vol. 40, pp. 1917-1941, 2010.

[5] W. E. Rogers, A. V. Babanin, and D. W. Wang, "Observation-Consistent Input and Whitecapping Dissipation in a Model for Wind-Generated Surface Waves: Description and Simple Calculations," *Journal of Atmospheric and Oceanic Technology*, vol. 29, pp. 1329-1346, 2012.

[6] R L Snyder, F W Dobson, J A Elliott, and R B Long, "Array measurements of atmospheric pressure fluctuations above surface gravity waves," *Journal of Fluid Mechanics*, vol. 102, pp. 1-59, 1981.

[7] O M Phillips, "On the generation of waves by turbulent wind," *Journal of Fluid Mechanics*, vol. 2, pp. 417-445, 1957.

[8] J W Miles, "On the generation of surface waves by shear flows," *Journal of Fluid Mechanics*, vol. 3, pp. 185-204, 1957.

[9] S. Hasselmann, K. Hasselmann, J. H. Allender, and T. P. Barnett, "Computations and Parameterizations of the Nonlinear Energy Transfer in a Gravity-Wave Spectrum. Part II: Parameterizations of the Nonlinear Energy Transfer for Application in Wave Models," *Journal of Physical Oceanography*, vol. 15, pp. 1378-1391, 1985.

[10] Klaus Hasselmann, "On the spectral dissipation of ocean waves due to white capping," *Boundary-Layer Meteorology*, vol. 6, pp. 107-127, 1974.

[11] Willard J. Pierson and Lionel Moskowitz, "A proposed spectral form for fully developed wind seas based on the similarity theory of S. A. Kitaigorodskii," *Journal of Geophysical Research*, vol. 69, pp. 5181-5190, 1964.

[12] G. J. Komen, S. Hasselmann, and K. Hasselmann, "On the Existence of a Fully Developed Wind-Sea Spectrum," *Journal of Physical Oceanography*, vol. 14, pp. 1271-1283, 1984.

[13] Peter A. E. M. Janssen, "Quasi-linear theory of wind wave generation applied to wave forecasting," *Journal of Physical Oceanography*, vol. 21, pp. 1631-1642, 1991.

[14] Heinz Günther, Susanne Hasselmann, and P. A. E. M. Janssen, "Report No. 4. The WAM Model Cycle 4," Hamburg, 1992.

[15] Rodolfo Bolaños, *Tormentas de oleaje en el Mediterráneo: Física y Predicción*. Barcelona, Spain: Universitat Politècnica de Catalunya, 2004.

[16] Jean Bidlot, Saleh Abdalla, and Peter Janssen, "A revised formulation for ocean wave dissipation in CY25R1," 2005.

[17] L. Bertotti and L. Cavaleri, "Large and small scale wave forecast in the Mediterranean Sea," *Natural Hazards and Earth System Sciences*, vol. 9, pp. 779-788, 2009.

[18] Marta Alomar, *Improving wave forecasting in variable wind conditions. The effect of ressolution and growth rate for the Catalan coast.* Barcelona: Universitat Politècnica de Catalunya, 2012.

[19] Hendrik L. Tolman and Dmitry Chalikov, "Source Terms in a Third-Generation Wind Wave Model," *Journal of Physical Oceanography*, vol. 26, pp. 2497-2518, 1996.

[20] N. Booij, R. C. Ris, and L. H. Holthuijsen, "A third-generation wave model for coastal regions: 1. Model description and validation," *Journal of Geophysical Research*, vol. 104, pp. 7649-7666, 1999.

Coastal and Ocean Modeling Testbed Applications

C. Reid Nichols [1)*], Robert G. Weisberg [2)] and André J. van der Westhuysen[3)]
[1)] Southeastern University Research Association, Washington, D.C.
[2)] University of South Florida
[3)] IMSG at NOAA/NWS/NCEP/Environmental Modeling Center, Maryland
[*]Corresponding author: rnichols@sura.org

Abstract—The Southeastern Universities Research Association (SURA) is involved in the research, development, and transition of ocean models from exploratory/advanced research to operations. The SURA Coastal and Ocean Modeling Testbed (COMT) program uses the science of collaboration to apply advances made by the coastal ocean modeling research community to improve operational ocean products and services. The long-range vision of the program is to increase the accuracy, reliability, and scope of operational coastal and ocean forecasting products. Accurately modeling surface gravity waves in the coastal ocean is especially important to help protect property and to save lives. This paper highlights recent advances in wave modeling by principal investigators that have supported the COMT program [1]. The four pillars of COMT are basic and applied research, technology transition, archival of discoverable information, and dissemination of data standards and software tools.

1. Introduction

A gravity wave field consists of a large number of single wave components each characterized by wave height, period, and direction [2]. Short waves such as wind waves and swell are modeled differently than long waves such as surf beats, seiches, tides, and tsunamis.

Wind wave modeling involves the use of numerical techniques to simulate sea states. Traditional wave models used by oceanographers and engineers are provided in Table 1. Wave models are forced by winds and include nonlinear wave interactions, whitecapping, depth induced wave breaking, and frictional dissipation. The model output generally consists of wave height, wave period, and direction statistics. The Coastal Ocean Modeling Testbed (COMT) program has run the Simulating WAves Nearshore (SWAN) model over large sections of the Eastern Atlantic Ocean, Caribbean Sea, and Gulf of Mexico as well as in several nearshore applications. Wave hindcasts and forecasts are extremely important for the maritime industry and coastal construction. For example, wave model output may be used to support vessel planning (e.g., docking, optimal ship tracking), search and rescue, forces on structures and for the further modeling of sediment transport, erosion, and accretion.

COMT has been especially important to understand variations in wave model results that may arise from differences in wind forcing and differences in parameterizations of physical processes. Future efforts may include data assimilation, and numerical techniques used to solve the wave action evolution equation.

Table 1. Wave Models

Name	Primary Use
WAVEWATCH III® (WW3)	Operational wave predictions, the current version includes shallow water parameters.
SWAN	Short crested waves in coastal and inland regions.
Delft3D	Short wave generation, sediment transport, morphological changes, ecological processes, and water quality
WW3 includes global and regional nested grids. SWAN has been run regionally and locally. Delft3D is often used to simulate local hydrodynamic conditions.	

2. Input

Wave models benefit from information derived from satellite altimeters, wave buoys, or other models to describe sea states. The COMT program continues to use data from networks such as the NDBC Ocean Observing System of Systems and the U.S. Integrated Ocean Observing System. Important data were collected from wave buoys, acoustic wave and current profilers, acoustic Doppler current profilers, and pressure sensors during tropical cyclones such as HUGO (1989), ANDREW (1992), MARILYN (1995), GEORGES (1998), LENNY (1999), KATRINA (2005), IKE (2008), ISAAC (2012), and SANDY (2012). The use of real data for exploring model parameter choices generally improves model skill as opposed to simply relying on boundary conditions obtained from previous forecasts or climatological data.

The wave model skill is especially sensitive to forcing by accurate wind fields. The desired input is a time-varying map of wind speed and directions. C-MAN Stations, NDBC buoys, remote sensors such as QuikSCAT, SSM/I or ERS2 and forecast models are all important sources of wind data. In the open ocean where there are significant wave current interactions, inputs should include reliable information on the total current (includes permanent currents, tidal, inertial, and hydraulic currents). In polar regions, waves are also affected by sea ice and icebergs. In shallow and intermediate depth the effect of bathymetry and islands must be considered. It is noted that many model applications do not include such effects, partly due to limitations associated with model resolution.

3. Representation

Waves are generally described as a spectrum, where the sea surface is decomposed into waves of varying frequencies using the principle of superposition. Waves are also separated by their direction of propagation. Model domains can range in size from local, regional to global scales. Smaller domains can be nested within a regional or global domain to provide higher resolution for a region of interest such as a coastal bay. The sea state evolves according to physical equations that are based on a spectral representation of the conservation of wave action. Calculations include wave propagation, advection, refraction (by bathymetry and currents), shoaling, and a source function which allows for wave energy to be augmented or diminished. Forcing generally includes wind forcing, nonlinear transfer, and dissipation by whitecapping. Wind and other atmospheric data are typically provided from a separate atmospheric model from an operational weather forecasting center. For intermediate water depths the effect of bottom friction should also be added. Further, for open ocean models dissipation of swells (without breaking) has been shown to be a very important term.

Spectral wave information can be used to support a variety of operations from coastal construction to offshore alternative power generation. Wave spectra are used in design criteria for shoreline protection structures. Coupled models can also be used to investigate whether or not structures such as groins and jetties will alter the natural processes of the beach, since these types of shore protection often lead to erosion on adjacent stretches of the coast, which also increases the risk of flooding. Representative ocean wave spectra may be used to generate time-series of wave surface displacement data for individual wave energy converters that are deployed in a wave park.

4. Output

The output from a wind wave model is a description of the wave spectra, with amplitudes associated with each frequency and incident wave direction. Results are typically summarized by the significant wave height, which is the average height of the one-third largest waves, and the period and incident direction of the dominant wave.

Data and information from the COMT collaboration website may be accessed from http://testbed.sura.org/datatable. As an example of data which could be used for severe weather planning are operational ocean wave predictions and wave buoy data from Hurricanes IKE (see Fig. 1 and Fig. 2) and GEORGES (see Fig. 3). Wave heights generated by IKE decrease as they propagate into shallow water owing to white capping, depth-induced wave breaking, and bottom dissipation [3]. As an example from the Caribbean Sea, are operational coastal surge and wave predictions and wave buoy data from Hurricane GEORGES, which made landfall on the SE of Puerto Rico. Significant surges were generated by GEORGES as the system moved over the reef shelf, strengthened by momentum transfer from wave breaking in shallow water [5].

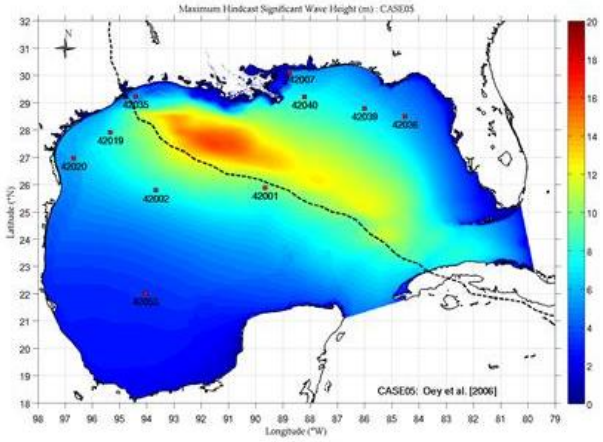

Figure 1. Model derived significant wave heights (m) during Hurricane IKE (2008) that re-strengthened in the Gulf of Mexico (obtained from [3]). Model output is in close agreement with NOAA's mid Gulf of Mexico 3-meter discus buoy.

5. Coupled Models

Coupled models may be used to support theoretical investigations of the mechanisms behind physical

phenomena from waves, tides, and shallow water processes to climatic change. Wind waves also act to modify currents and atmospheric properties through frictional drag of near-surface winds and heat fluxes. Two-way coupled models allow the wave activity to feed back into the circulation and upon the atmosphere. An example U.S. Geological Survey project that is focused on understanding coastal erosion is the Coupled Ocean – Atmosphere – Wave – Sediment –

Figure 2. NDBC Station Number 42001. 3-meter discus buoy moored in the mid Gulf of Mexico, 180 nm south of Southwest Pass, LA at a depth of 3,365m. A maximum significant wave height of 9.25m was observed at 12:50 PM CST on September 8, 2008 during Hurricane IKE.

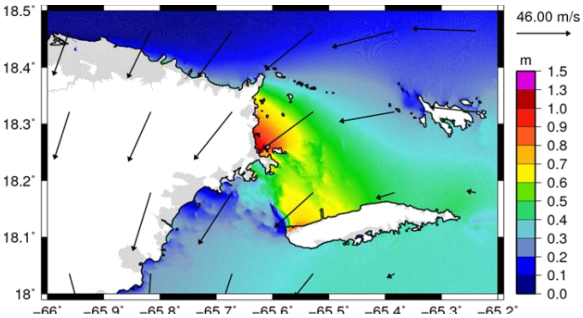

Figure 3. Model-derived coastal surge (m) during Hurricane GEORGES (1998) over the SE of Puerto Rico and the island of Vieques. Arrows indicate wind velocity vectors (obtained from [5]).

-Transport (COAWST) modeling system [6]. Coupled models such as COAWST allow researchers to simulate interactions between foreshore, nearshore, and offshore sediment transport processes. Information from the Weather Research and Forecasting model, Regional Ocean Modeling System, SWAN, and the Community Sediment Transport Modeling Project [7] are integrated by COAWST. Several examples of coupled models used during the COMT project are listed in Table 2. Future researchers may use coupled models to separate natural variability from anthropogenic effects, which would be especially useful to mitigate the effects of sea level rise.

Table 2. Coupled models.

Model System	**Benefits**
FVCOM+SWAN	Deep and shallow surface waves
ADCIRC+SWAN	Characterizing storm surge
SLOSH+SWAN	Coastal surge analysis
Delft3D+SWAN	Water flow and waves
ADCIRC+ *WAVEWATCH III*®	Improve nearshore simulations of inundation
The added features obtained through coupling are helping to generate actionable surge information.	

Numerous researchers, e.g., [1], [3], and [8], working with COMT have applied wave (e.g., SWAN and *WAVEWATCH III*®) and circulation (e.g., ADCIRC, FVCOM, and SELFE) models to produce timely products characterizing extreme events that support decision makers. Comparisons of the above coupled wave and circulation models to observations (e.g., tide gage data) during nor'easters have showed similar accuracies.

Archives that highlight wave heights and breaking waves during storms, storm surge during the passage of hurricanes, or river and coastal inlet plumes in synchronization with favorable winds are especially useful for contingency planning and coastal zone management. The COMT archive is intended to help validate new models that can be run for future events or other purposes. The COMT archive may allow data innovators, who want to use model output to develop integrated products, to help operators anticipate the impacts of extreme events. COMT output can support exercises that help Commanders determine when to sortie Navy Ships from Homeports to avoid hurricanes such as SANDY that occurred during 2012.

6. Verification

The verification of coastal wave models is challenged by factors such as changing wind fields, shoreline shape, and bathymetry. Thus, coastal systems are

not closed and the ensuing model results are specific to selected times and spaces. Model results can be confirmed through comparison with observations and other models, but the intercomparison is inherently limited. Therefore, their predictive value should be continuously evaluated.

COMT provides an archive of observational data and model output during significant historical coastal flooding events. Important input, output, and representations are provided to support model comparisons. Since the extent of inundation is a function of factors such as inland topography, vegetation, geomorphology, and coastal structures, geospatial information is provided in the archive. Such information is especially helpful to understand direct inundation (the water level exceeds the land elevation), overtopping (water flowing over berms, dunes, and other barriers), and breaching (barriers are broken by waves). This combined information is important to determine different inundation paths.

The archive includes input data, model output, and/or observational data that can be used for skill assessments. Future efforts may explore using this information to support contingency planning (e.g., marine spill response, search and rescue, and use to support marine operations such as trans-ocean tows of large structures). The archive has been produced using the oceanographic community's leading numerical models, whose outputs in some applications characterized important phenomena such as inundation, waves in a seaway, and sediment transport.

7. Reanalysis

Historic data and archived model output are useful for a variety of scientific applications. Hindcasts involve the use of historical data (or closely estimated inputs for past events) to assess how well output matches known results. A retrospective analysis may also be conducted by combining all available observations with a physical model to describe the model domain over decades. One might use wave observations from the International Comprehensive Ocean Atmosphere Data Set (ICOADS) and other models to build monthly, interannual, and multi-decadal wave climatologies or atlases.

The COMT program included the comparison of sea level and waves for four regional-scale models, i.e., ADCIRC+SWAN, SLOSH+SWAN, Delft3D+SWAN, and ADCIRC+WAVEWATCH III® in the Caribbean Sea. These intercomparisons highlighted the importance of using hindcast best winds rather than a parametric wind model. Further, this research highlighted improvements in SLOSH modeling of inundation by incorporating wave effects from a parametric wave model in its surge calculations.

8. Applications

Coastal flooding is largely a natural event, however human influence on the coastal environment can alleviate or exacerbate the negative consequences. NOAA reports that a majority of U.S. coastal areas will face 30 or more days of flooding each year due to impacts from sea level rise by 2050 [9]. For this reason, COMT archives might be developed to support resilience assessments in locations such as those listed in Table 3. COMT can use model output and data such as NOAA water level records to investigate and qualify the influence of sea level rise on inundation.

This research is especially important to planners responsible to mitigate the effects of coastal flooding, especially increases in nuisance flooding that is currently being experienced as a consequence of sea level rise.

Table 3. Key locations for resilience assessments.

Geographic Location	Affected City
Mid Atlantic Bight	Boston, MA; New York, NY; Philadelphia, PA; Baltimore, MD; and Washington, D.C.
South Atlantic Bight	Norfolk, VA; Wilmington, NC; and Charleston, SC
Gulf of Mexico	New Orleans, LA; Tampa, FL; Houston & Corpus Christi, TX.
Caribbean	*Puerto Rico*, northern U.S. Virgin Islands, Naval Station Guantanamo Bay
West Coast	Bremerton, WA; Holy Cross, WA; Longview, WA; Bay City, OR; Portland, Oregon; Petaluma, CA; Los Angeles, CA, and San Francisco, CA
Flooding and inundation is a concern for small, low and flat islands, especially coral atolls that are found in the Caribbean (~ 15) and Pacific (~ 400). These islands are highly vulnerable to elevated sea levels caused by tropical cyclones.	

Communities that are particularly vulnerable to in-

undation and flooding will find that combined access to historical information (e.g., water level fluctuations), *in-situ* data (wave buoy records and hydrographic surveys), imagery (waterlines and digital elevation models), and numerical model output (spatially extensive) are essential to effective risk management and assessing resiliency. COMT will ultimately provide an archive for selected sites that could be used as another tool to develop plans to reduce vulnerabilities and adapt to change. SURA is presently planning to use the archive to develop scenarios that help planners ensure that they are resilient against future flooding and inundation events.

SURA's role in collaborative science ensures that it remains knowledgeable on state-of-the-art ocean and atmospheric modeling efforts, and can make recommendations to operational organizations such as NOAA concerning model issues, transition processes, and policy. SURA has ongoing plans to provide model assessments for the NOAA Integrated Ocean Observing System and government-university-industry partnerships involved with coastal resilience. Primary tasks help to assess and coordinate planned wave model transitions from exploratory/advanced development to operational status to ensure coherent program integration. The COMT program helps to ensure a systematic and efficient transition approach is maintained for wave and circulation models.

SURA also intends to develop the COMT archive to support mitigation decisions that could range from moving critical infrastructure farther inland to developing environmentally sustainable shore protection.

9. Conclusions

The COMT Program works collaboratively with partners from government, academia, and the private sector. Scientific communications (e.g., [1], [3], [4], [10], and [11]) are used to recommend ocean/atmosphere modeling techniques and data assimilation priorities for operational use.

Model comparisons with Integrated Ocean Observing Systems that include wave buoys, ocean current and surface meteorology buoys, tide stations, and other ocean and atmosphere observations are critical. In some locations, where there are data gaps, model simulations are especially important to provide planners with spatially extensive information on waves, flooding, and inundation.

Future efforts by the SURA COMT should support the review, quantitative verification, and gap analyses of model transition plans (general and specific) in the ongoing demonstration and operational implementation phases. COMT archives should be designed to ensure that model output and associated transition plans are responsive to operational needs.

10. Acknowledgment

This work has been sponsored by the NOAA Integrated Ocean Observing System (IOOS®) under Zdenka Willis and Becky Baltes, as well as partner contributions from the U.S. Army Corps of Engineers, U.S. Geological Survey, National Hurricane Center, and the Caribbean Coastal Ocean Observing System. Key results have been made by researchers from University of Notre Dame, University of Puerto Rico, and University of South Florida. We would also like to acknowledge the review and edits by Drs. Robert Williams, Don Wright, and Rick Luettich whose scientific insights enhance the final product.

11. References

[1] Luettich, R.A., L.D. Wright, R. Signell, C. Friedrichs, M Friedrichs, J. Harding, K. Fennel, E. Howlett, S. Graves, E. Smith, G. Crane, and R. Baltes, 2013, Introduction to Special Section on the U.S. IOOS Coastal and Ocean Modeling Testbed, J. Geophys. Res. Oceans, 118, pp 1-10.

[2] Nichols, C.R., and R.G. Williams. Encyclopedia of Marine Science. New York: Facts On File, 2009

[3] Huang, Y., R. H. Weisberg, L. Zheng and M. Zijlema (2013), Gulf of Mexico hurricane wave simulations using SWAN: Bulk formula based drag coefficient sensitivity for Hurricane Ike. J. Geophys. Res., 2012JC008451, doi: 10.1002/jgrc.20283.

[4] Zheng, L, R.H. Weisberg, Y. Huang, R.A. Luettich, J.J. Westerink, P.C. Kerr, A. Donahue, G. Crane, and L. Akli (2013), Implications from Comparisons Two and Three Dimensional Model Simulations for the Storm Surge of Hurricane Ike. J. Geophys. Res., 2013JC008861, doi: 10.1002/jgrc.20248

[5] Andre J. van der Westhuysen et al. A Wave, Surge, and Inundation Modeling Testbed for Puerto Rico and the U.S. Virgin Islands: Year 1 progress. In: 95th AMS Annual Meeting, Phoenix, AZ, 4–8 January 2015.

[6] COAWST: A Coupled-Ocean-Atmosphere-Wave-Sediment Transport Modeling System, Woods Hole Coastal and Marine Science Center, United States Geological Survey, Available online. URL: http://woodshole.er.usgs.gov/operations/modeling/COAWST/. Accessed December 30,2014.

[7] Community Model for Coastal Sediment Transport. Woods Hole Coastal and Marine Science Center, United States Geological Survey, Available online. URL: http://woodshole.er.usgs.gov/project-pages/sediment-transport/. Accessed December 30, 2014.

[8] Chen, C., R.C. Beardsley, R.A. Luettich Jr., J.J. Westerink, H. Wang, W. Perrie, Q. Xu, A.S. Donahue, J. Qi, H. Lin, L. Zhao, P.C. Kerr, Y. Meng, B. Toulany, 2013. Extratropical storm inundation testbed: Intermodel comparisons in Scituate, Massachusetts, Geophys. Res., 118, 5054-5073, doi:10.1002/jgrc.20397.

[9] Sweet, W. and J. Park, 2014. From the extreme to the mean: Acceleration and tipping points of coastal inundation from sea level rise. Available online. URL: **http://onlinelibrary.wiley.com/enhanced/doi/10.1002/2014EF000272/**. Accessed on December 20, 2014.

[10] SURA. Workshop entitled, "Understanding and Modeling Risk and Resilience in Complex Coastal Systems," October 29 & 30, 2014, Southeastern Universities Research Association, 1201 New York Ave. NW, Washington, D.C.

[11] Luettich, R.A. et al. The IOOS / SURA Coastal and Ocean Modeling Testbed (COMT). A Wave, Surge, and Inundation Modeling Testbed for Puerto Rico and the U.S. Virgin Islands: Year 1 progress. In: 95th AMS Annual Meeting, Phoenix, AZ, 4–8 January 2015.

Session II Presentation

The Session II Presentation can be accessed online at URL:

http://scholarworks.uno.edu/oceanwaves/2015/Session2/

Session II Notes

Recent Developments in wave modeling with applications for operations

These notes are intended as a supplement to the presentation, "Energetic Surface Waves Measured in Arctic Ice." The following discussion points were captured by workshop rapporteurs:

- As researchers assess impacts from the possibility of an ice free Arctic, a new area for coupled modeling involves wave growth and dissipation along ice edges and leads. The interaction of waves with retreating ice reduces ice cover, which in turn increases wave fetch.

- Waves and sea-ice interactions are complex. The sea ice has an impact on the wave field, but the wave field also has an impact on the sea ice.

- Seasonal sea ice is much weaker than long-term (multi-years old) ice.

- Large waves generated in open water propagate through ice and this phenomenon may be happening on a regular basis. Ice begins to break up very quickly owing to wave propagation. Initially sea ice responds mainly to low frequency waves, but as the ice breaks up, higher frequencies prevail.

- Assessments of wave growth in ice may be studied using outside wave tanks such as Ohmsett, the National Oil Spill Response Test Facility. Ohmsett is the largest outdoor saltwater wave/tow tank facility in North America.

- Model verification requirements are dependent upon model resolution and benefit from higher and more uniform spatial coverage of wave observations.

- In some cases, organizations such U.S. Integrated Ocean Observing System, (IOOS®) have enhanced observatories with wave buoy deployments in the coastal ocean.

- Improved spectral observations can be used to better represent swell in wave forecast models.

- Wave observations are being used for assimilation into wave forecast models and verification of wave forecast models. Examples include operational assimilation of altimetry into WAVEWATCH III by Fleet Numerical Meteorology and Oceanography Center and planned data assimilation within a coupling project at NRL Stennis. Similar initiatives are underway

at the National Center for Environmental Prediction and the European Centre for Medium-Range Weather Forecasts.

- Verified wave models are essential to understand ocean wave climate and its variability on seasonal to decadal time scales. Observations are crucial to this understanding.

- Increasing the number of directional wave measurements to support WAVCIS will directly lead to improvements in Gulf of Mexico wave modeling technologies and will translate into better wave forecasting techniques for others.

- Wave buoys and models are important to improving our understanding of the role of waves in ocean-atmosphere coupling.

- Ship observations, especially from Polar Regions, may be useful to assessing wave processes and climatic conditions. Databases such as the International Comprehensive Ocean-Atmosphere Data Set (ICOADS) may be particularly useful in the development of climatologies and research on changing ice fields.

Session III – Advances and issues in wave measurement technologies

Today, ocean waves are observed and modeled using different sensors and numerical methods. Submerged instruments include combinations of current and pressure recorders mounted on fixed frames or on subsurface floats. At the ocean surface, state-of-the-art wave buoys may be used to measure the surface elevation and tilt. On piers and fixed platforms, wavestaffs, radar, and laser altimeters may also be employed. From overhead regions, remote sensing techniques may employ scanning radars, lasers, and scatterometers. Numerical models are also developing to assimilate observations and account for complications arising from waves either entering or being generated in finite depth or shallow waters. Advances are being made in the merging of disparate data that are received from the various types of observations and models. The following papers describe uses of wave information and impacts on surveying and in naval architecture.

Extended Abstracts

INTENTIONALLY BLANK

3D Imaging to Identify Scour and Beach Morphology

Blair Cunningham [1)*]
[1)] Coda Octopus Products Inc., Lakeland FL
[*]Corresponding author: blair.cunningham@codaoctopus.com

1. Introduction

Coda Octopus is the patent holder for the real time 3D sonar, the Echoscope®. Resulting bathymetric data can be used for numerical modeling of wave climate; sediment transport; tidal currents; and hydraulic currents.

The Echoscope® is a volumetric sonar that produces high resolution real-time 3D imaging. Complete 3D imagery is composed of over 16,000 data points, from each acoustic transmission in real time up to 12 times per second. With data densities far in excess of those generated by other sonars, the top-end visualization software takes advantage of patented statistical rendering techniques to enhance image clarity and detail, presenting an intuitive and easy-to-interpret image. When monitoring underwater activity, even when the target and the Echoscope® are moving independently of each other, the 3D imagery uniquely remains clear and accurate, giving the viewer an instant three-dimensional understanding of the underwater environment during operations. In dynamic survey and mapping tasks such as seafloor cable or pipeline inspections or scour monitoring, the ping geometry allows a target to be visualized many times in a single pass, with each view taken from a different angle. As a result more details and fewer shadows are seen, enabling mapping of complex subsea structures with a higher level of confidence and far more detail than can be achieved using alternative methods. A real-time view allows the operator to immediately make decisions to get a better view or to slow and take a "closer look" when he sees something of interest. With a navigation and attitude and positioning input, roll and pitch conditions are compensated for and an accurate geo-referenced measurable 3D data set is provided. This technology adds significant value to subsea inspections, marine structure inspections, archaeological surveys, and salvage operations.

Understanding the effects of scour around subsea structures such as seawalls, outfall piping and seafloor cables is critical for planning placement of protection and periodic maintenance (see Fig. 1). It is important for the survey to identify the current condition and provide data to understand variations over time due to seasonal events or tidal changes that can be critical to planning. Echoscope® provides a detailed, easy to understand assessment of scour conditions. Currently, it is being used in Brazil for underwater subsea sonar imaging and mapping to monitor erosion in the terrain surrounding pier piles and the morphology of the seabed attributable to the presence of vessels using the facility. These data are used determine scour changes over time and seasons so that computer models can be updated with actual data assessments. The data produced by the Echoscope® can be output in a XYZI RGB format and can be input into a GIS for further evaluation.

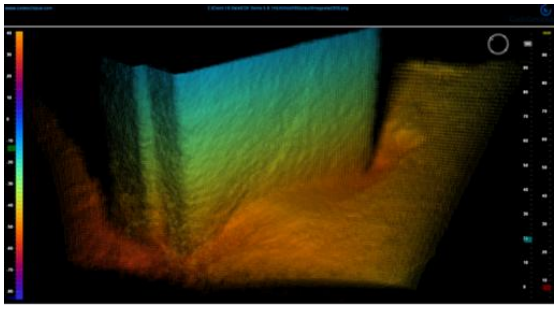

Figure 11. Main St. Bridge Jacksonville Florida depicting shoaling and scour

The Echoscope® has been shown to be capable of comfortably achieving bathymetric survey data that meet the various orders of IHO S-44 standards under typical survey conditions. Through the use of the post-processing steps in its Underwater Survey Explorer software package the data can further meet the highest of these orders (Special Order).

2. Conclusions

The Echoscope® can provide a detailed, easy to understand 3D image and bathymetric survey showing scour and morphology near and around subsea objects, near beach zones and seawalls. The IHO quality bathymetric data can be output to geodatabases for further evaluation and understanding of these conditions. Using its unique real-time visualization mode allows complete time-lapse monitoring of scour flow for detailed analysis. High resolution surveying could be used to quantify channel shoaling rates and as bathymetric data to develop improved numerical modeling grids.

Existing data processing strategies work to minimize the effect of rough water on data accuracy, but the effect on the collection crew must be considered especially in shallow water.

Long-term Observations of Tidal and Storm Surge Waves and Weather Associated Flushing of Louisiana Bays

Chunyan Li*, Baozhu Liu, Eddie Weeks, Bill Gibson, Steven Jones, Brian Milan, and DeWitt Braud
WAVCIS, Department of Oceanography and Coastal Sciences, Coastal Studies Institute, School of the Coast and Environment, Louisiana State University, Baton Rouge, LA
*Corresponding author: cli@lsu.edu

1. Introduction

Tidal waves and storm surges are usually amplified in the shallow water areas along the coast. Their impact to the coastal inundation and flushing of estuaries and bays is therefore significant, especially in a region where the land and shelf have only small gradients in elevation. The impact is further complicated by the weather systems in the region: hurricanes during the hurricane season (June to November) and winter storms ([1]-[5]) between the Fall and Spring (~October to April). Although hurricanes occur only sporadically and are limited to relatively small areas mostly within the radius of maximum wind, the local damages can be quite significant. The winter storms, even though less severe for the most part, occur from 20 to 30 times from mid-autumn to late spring every year and with a much larger spatial scale (~ 1000 km). These atmospheric activities acting on the water have implications to the land-ocean exchange, land-estuary exchange, and bay-ocean exchange in water, salt, nutrients, sediment, and other suspended and dissolved substances and the fate and activities of plankton and fish.

In the Louisiana coastal water, semi-enclosed bays are separated from the coastal ocean by a series of barrier islands. Water exchange occurs through narrow tidal inlets. As discussed in [3], winter storms can produce significant exchange flows in a multi-inlet system, in which some inlet(s) may experience inward flows while the rest experience outward flows. This may be dynamic and can change with conditions.

The continuous quantification of storm surge waves caused by either the summer or winter storms under the influences of tides is usually practiced without some of the required major parameters: usually only the water levels are measured but not the current velocity. The oscillation and flushing of bays under severe weather conditions can be quantified more completely by measurements of water velocity across all the tidal inlets. Our work involves the very first of its kind to measure continuously the flows across all the major inlets of the Barataria Bay of Louisiana.

2. Methods

To accomplish our objective of continuous measurements of flows across all the major inlets, i.e., Barataria Pass, Caminada Pass, and Pass Abel, we used several different horizontal acoustic Doppler current profilers (Sontek Argonaut, RD Instruments HADCP, and Nortek Awac), or ADCPs. For each ADCP, we used a lead acid battery charged by a 60 W solar panel through a solar controller. The data were saved every 5-20 minutes, depending on the deployment. Deployments usually lasted 2-3 months before a data download was made. If biofouling was observed, the ADCP was recovered for cleanup. The deployment roughly covered the period from August 2013 to July 2014; on December 19, 2014 sampling was restarted since there was a data gap of 146 days after July 2014 owing to a technical error in the setup. The data however are unique and support examination of flushing in the multi-inlet bay under tidal waves and severe weather, thereby providing insights to the weather induced hydrodynamic processes important to the geomorphology and land-ocean exchanges.

3. References

[1] Feng, Z., and Li, C., 2010. Cold-front-induced flushing of the Louisiana Bays. *Journal of Marine Systems*, 82, 252–264.

[2] Li, C.; Roberts, H.H.; Stone, G.; Weeks, E., and Luo, Y., 2011. Wind surge and saltwater intrusion in Atchafalaya Bay under onshore winds prior to cold front passage, *Hydrobiologia*, 658, 27–39, DOI 10.1007/s10750-010-0467-5.

[3] Li, C. and Chen, C., 2014. Shelf circulation prior to and post a cold front event measured from vessel-based acoustic Doppler current profiler. *Journal of Marine System*, 139, 38-50.

[4] Roberts, H.H., 1998. Delta switching: Early impacts on the Atchafalaya River diversion. *Journal of Coastal Research*, 14, 882-899.

[5] Walker, N.D. and Hammack, A.B., 2000. Impacts of winter storms on circulation and sediment transport. Atchafalaya-Vermillion Bay Region, Louisiana, U.S.A., *Journal of Coastal Research*, 16, 996-1010.

The Harold E. Saunders Maneuvering and Seakeeping (MASK) Facility New Directional Wavemaker

John G. Hoyt III [1)*], Scott Carpenter [2)]
[1)] CSC, West Bethesda, MD
[2)] Naval Surface Warfare Center, Carderock Division, West Bethesda, MD
Corresponding author: jhoytiii@csc.com

Abstract—The Naval Surface Warfare Center (NSWC), Carderock Division (Fig. 1) has modernized, through replacement, their pneumatic type wavemaker (Fig.1). The original design dates back to the mid 1940's and was constructed in the late 1950's in Bldg 18 that houses both the Maneuvering and Seakeeping Basin and the Rotating Arm Facilities (Fig. 2).

Figure 1. David Taylor Model Basin

1:120 Scale Model of Rotating Arm and Maneuvering Basin

Figure 2. Original schematic of David Taylor Model Basin (see [1]).

A contract was awarded in 2007 to MAR Inc. to lead a team consisting of Edinburgh Design Limited (wavemaker designer), Atlantic Industrial Technologies (Machinery Fabrication and Engineering Design), INCON (Installation of Machine and Structural and Electrical Support Components) and McLaren Associates (Design and Inspection of Concrete Support Structure). This 216 paddle directional wavemaker was designed, installed and completed in the fall of 2013.

This wavemaker has 216 pivoting paddles along two sides of the basin. Each paddle is 0.658 m wide, with a hinge depth of 2.5 m (Fig. 3). It is dryback type, driven by electric motors through a timing belt on a curved sector. The hydrostatic force of the water on the wave paddle faces is compensated for with air springs. The waves are generated using an energy algorithm using paddle force as the primary feedback. An additional design feature of this wavemaker is the use of a curved corner to minimize the singularity that would be created if a square one was used (Fig 4.).

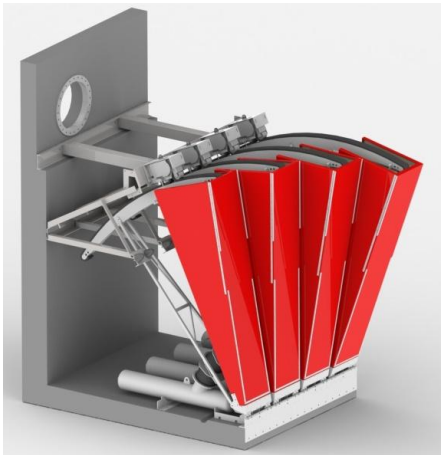

Figure 3. Wavemaker Paddle Design

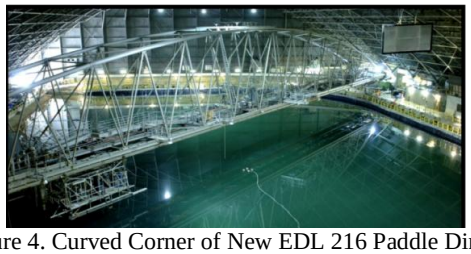

Figure 4. Curved Corner of New EDL 216 Paddle Directional Wavemaker

This wavemaker is capable of producing regular and random directional waves. Using the directional capability deterministic and focused wave events can be simulated. These events can be viewed using the "Virtual Wavemaker" that visualizes the wave time history that is requested on the computer screen.

Details of the wavemaker design, control and capabilities are presented with a presentation showing the time lapsed history of construction and demonstration of its capability are presented.

References

[1] Naval Surface Warfare Center Carderock Division. Available online. URL: www.navsea.navy.mil/nswc/carderock/default.aspx. Accessed on December 19, 2014.

INTENTIONALLY BLANK

The Harold E. Saunders Maneuvering and Seakeeping (MASK) Facility New Directional Wavemaker

John G. Hoyt III [1)*], Dan Hayden [2)], Scott Carpenter [2)]
[1)] CSC, West Bethesda, MD
[2)] Naval Surface Warfare Center, Carderock Division, West Bethesda, MD
Corresponding author: jhoytiii@csc.com

Abstract— The Naval Surface Warfare Center, Carderock Division has modernized their pneumatic type wavemaker. The original design dates back to the mid 1940's, was constructed in the late 1950's and is located in Building 18 that houses both the Maneuvering and Seakeeping Basin (MASK) and the Rotating Arm Facilities.

In 2007, a contract was awarded to MAR Inc. who led a team consisting of Edinburgh Design Limited, Atlantic Industrial Technologies, INCON and McLaren Associates to design, construct and install the new wavemaker. The project, design, construction and installation was completed in the fall of 2013.

This wavemaker has 216 pivoting paddles along two adjacent sides of the basin. Each paddle is 0.658 m wide, with a hinge depth of 2.5 m. It is dry-back type, driven by electric motors through a timing belt on a curved sector. The hydrostatic force of the water on the wave paddle faces are compensated for with air springs. The waves are generated using an energy algorithm using paddle force as the primary feedback.

Two additional design features of this wavemaker. First a curved corner, used to minimize the singularity that is created with a square one as was used in the pneumatic design. Second a control algorithm is applied that not only generates the commanded waveform, but also attempts to absorb any unwanted background wave energy such as beach reflections, model wake and most importantly second order self-generated cross board wave.

This wavemaker is capable of producing regular waves at oblique angles to the wave banks as well as long crested and short crested irregular model seas. Using the directional capability, deterministic and focused wave events can be simulated. Multi Directional waves with spreading modeling such things as a local sea and swell can now be modeled.

Another powerful capability of the new system is the ability to preview the commanded waves in 3D virtual space on the computer screen. In this way, the test engineer can, prior to running the wavemaker, view the model sea. The test team is now able to make decisions relative to the placement of the model, course and direction, in order to maximize the interaction with the modeled seaway.

1. Introduction

In 2006, The Naval Surface Warfare Center, Carderock Division (NSWCCD) (Fig. 1) began a study that led to a "White Paper" stating the need for new wavemaking systems for the Maneuvering and Seakeeping Basin (MASK), High Speed and Deep Towing Basins. These original pneumatic wavemakers are designs that date back to the mid 1940's, the newest, MASK, being constructed in the late 1950's and located in Building 18 that houses both the MASK and the Rotating Arm Facilities (Fig. 2).

Figure 1. David Taylor Model Basin

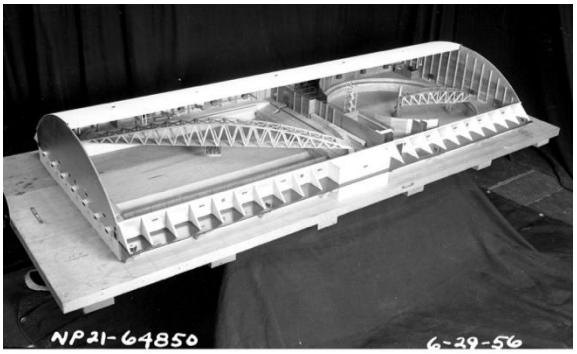

Figure 2. Rotating Arm and Maneuvering and Seakeeping Basin.

The major argument for the need of the Navy to modernize their wavemaking capability was to create the ability to test in short crested seas. The existing pneumatic wavemakers, although simple and easy to

maintain, as testified by their length of service, were too difficult to control to produce wave spectra envisioned for future testing - let alone short crested directional seas. Given the age of the three wavemaking systems and the need for refurbishment to reduce down time and restore original wavemaking capability lost due to aged hydraulics, modernization through replacement to new and more easily controllable machines was proposed.

In 2007 a contract was awarded to MAR Inc. to lead a team (Fig. 3) consisting of Edinburgh Design Limited (wavemaker designer), Atlantic Industrial Technologies (Machinery Fabrication and Engineering Design), INCON (Installation of Machine and Structural and Electrical Support Components) and McLaren Associates (Design and Inspection of Concrete Support Structure).

Figure 3. Wavemaker Team

Edinburgh Design Limited (EDL) designed a segmented dryback directional wavemaker for the MASK (Fig. 4). This design promised the same capacity in achievable wave heights and frequency range as well as the ability to skew the wave fronts and with the software under development by EDL, the ability to produce multiple irregular seaways with or without spreading.

For the Deep (Fig. 5) and High Speed Basins (Fig. 6), segmented variable depth wavemakers were proposed. A segmented and dryback design was used to allow interchangeability of parts, and make it possible to use the same control software architecture in all wavemaking systems.

Since the Deep Basin wavemaker divided the wide basin into a shallow and deep end, it needed to be able to "tuck" down under a towing carriage if ever it was required on the other side. This opened the doors for the variable depth capability. Retaining segmentation allows the production of more linear wave fronts in the basins and reduction of the so-called serpentine waves often produced near the tank width resonance.

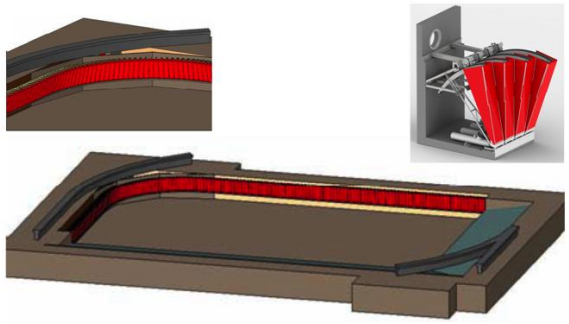
Figure 4. EDL MASK Wavemaker Design.

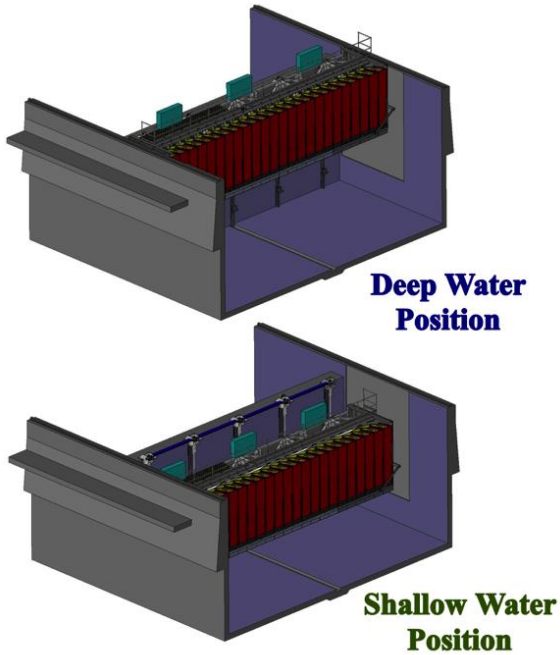

Figure 5. EDL Deep Basin Wavemaker Design.

The Navy decided to fund the design of all wavemakers and the construction of the MASK system. The MASK wavemaker was installed and completed in the fall of 2013 (Figs. 7) and is currently

being used to support a future Naval Surface Ship Combatant.

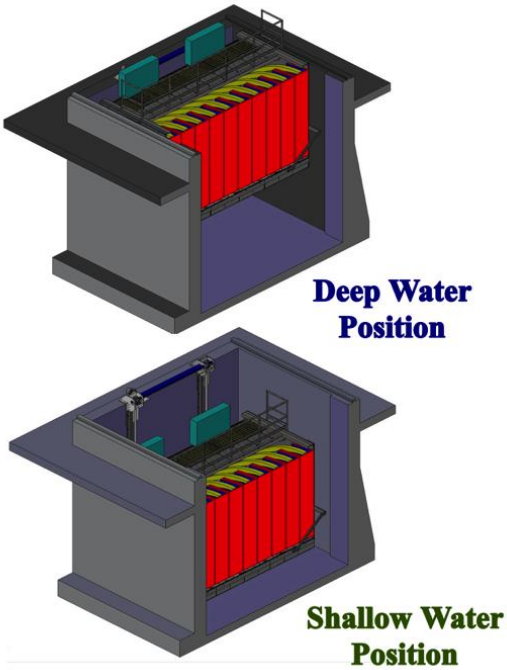

Figure 6. EDL Wavemaker Design

Figure 7. Curved Corner of EDL 216 Paddle Directional Wavemaker

2. History

NCWCCD can trace its own roots to the Experimental Model Basin (EMB) built by then Captain David W. Taylor (Fig. 8) at the Navy Yard in Washington, DC (Fig. 9). This flap type wavemaker was moved into the 140 ft basin in 1940. It was first used as a flap wavemaker and then was cannibalized to provide the drive mechanism for early prototypes of pneumatic type wavemakers in 1950 (Fig. 10).

Pneumatic wavemakers were installed in both the Deep and High Speed Basins in the early 1950's (Fig. 11). Immediately work began on the design of a seakeeping basin that would become the MASK. A 1/10th scale model of the MASK was built and tested at the then David Taylor Model Basin (Fig. 12). This facility was given to the University of Michigan where it was used by the Naval Architecture Department (see http://name.engin.umich.edu/).

RADM David Watson Taylor, *USN Retired (1864 - 1940) was a naval architect and engineer of the United States Navy. He graduated with the highest grade average in U.S. Naval Academy history. He served during World War I as Chief Constructor of the Navy, and Chief of the Bureau of Construction and Repair. Taylor is best known as the man who constructed the first experimental towing tank ever built in the United States. The Navy's Research and Development community honored Taylor by naming its new model basin, constructed at Carderock, Maryland, after him. The Model Basin retains his name as a living memorial to this distinguished naval architect and marine engineer.*

Figure 8. Admiral David W. Taylor.

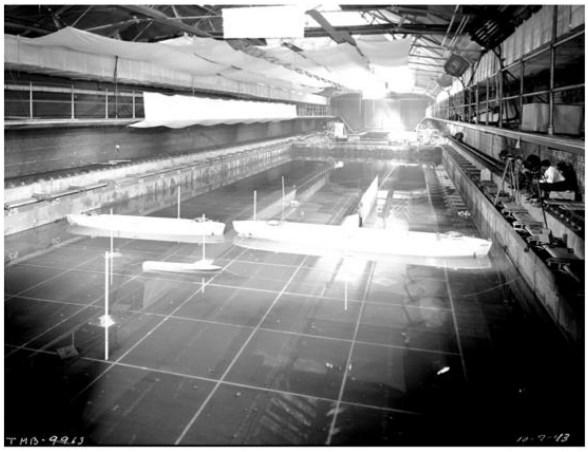

Figure 9. Navy's 1st Flap Wavemaker in the Experimental Model Basin (1913).

Looking at Figure 12 it is interesting to take note of the non-uniformity along the wave fronts. There were 21 total wave domes in the old pneumatic MASK wavemaker. The west bank held 8 domes and the north bank 13. In the far field, each dome is generating a ring wave. Although it appears that the wave front produced by, in this case eight wave domes, has

a lack of uniformity caused primarily by the second order cross tank energy as well as the reflections of both the beach and adjacent static wavemaker. The use of force feedback and wave absorption has greatly improved the uniformity in the basin.

Figure 10. Pneumatic Prototypes Developed in the 140ft Basin.

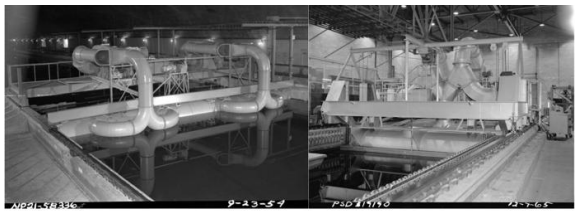

Figure 11. Pneumatic Wavemakers Located in the Deep and High Speed Basins.

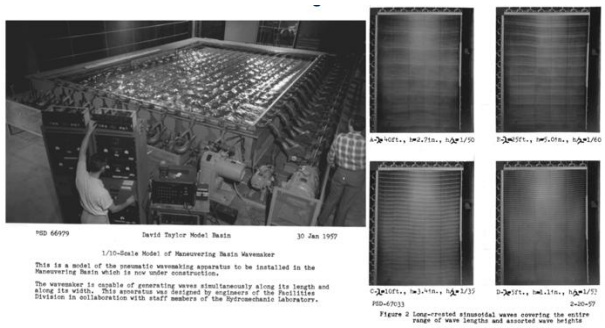

Figure 12. 1/10th Scale Model of the MASK Basin.

The Harold E. Saunders Maneuvering and Seakeeping Basin (MASK) was placed into service in 1961, being named for Captain Saunders (Fig. 13). Its wavemaking system comprised of two banks of 21 ft wide pneumatic domes, as previously stated 8 on the west bank and 13 in the north bank (Fig. 14). The pneumatic design was chosen because of its promise of lower maintenance costs. This promise has been made good over the years.

The original MASK wavemaker used a shaft line drive driven by a "Scotch Yoke" arrangement to convert the rotary motion of the hydraulically driven line shafts in to reciprocal motion to move the control flappers that regulated the pressure created in the domes by centrifugal blowers. The west or short bank was changed during construction to independent hydraulic actuator control to permit study into the generation and testing of ship models in irregular waves. It is interesting to note that the original "Scotch Yoke" line drive could be indexed to phase the domes to skew the wave front. However, with a dome width of 21 ft, the angle achievable was limited.

Captain Harold Eugene Saunders, USN Retired (1890–1961) was a distinguished career Naval officer. He graduated with the second highest grade average in U.S. Naval Academy history, second to David W. Taylor. He served at the Portsmouth, New Hampshire Navy yard and was involved in the design and construction of submarines. He received the Navy Distinguished Service Medal for his work in salvaging the USS-4 (SS-109) in 1927. Saunders was a member of the first and second Byrd expeditions to Antarctica, where he served as a geographer. The Saunders Ice Shelf, Saunders Coast, and Saunders Mountain are named for him. He is best known for being the Chief Constructor of the David Taylor Model Basin. He authored the 3-volume book, Hydrodynamics in Ship Design, which was published in 1957 by SNAME. The Maneuvering And Seakeeping Basin retains his name as a living memorial to this distinguished naval architect and marine engineer.

Figure 13. Captain Harold E. Saunders

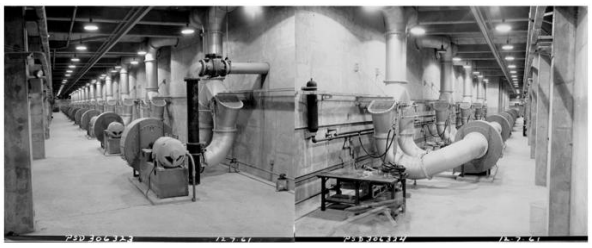

Figure 14. MASK Pneumatic Drive Lines.

This wavemaker was refurbished in the mid 1980's replacing both banks with independent MTS Inc. hydraulic actuation. It has been a good and reliable machine.

3. Design

The MASK wavemaker was reliable; however it had severe limitations on its ability to produce model sea spectra especially at frequencies above 1.4 Hz. The system was essentially a spring mass system that was

very under damped with a very soft spring (the air column) making it extremely non-linear.

Wave spectra are produced then and now through an iteration process, i.e, an initial drive history is created, a transfer function assumed and then, through a trial and error procedure, modified until the desired spectral shape is obtained.

This iterative process could take as many as 7 or 9 iterations adding days to the test time and commensurate cost. A single universal transfer was never found due the nonlinear interactions of the machine (Fig. 15). And directional wave were out of the question.

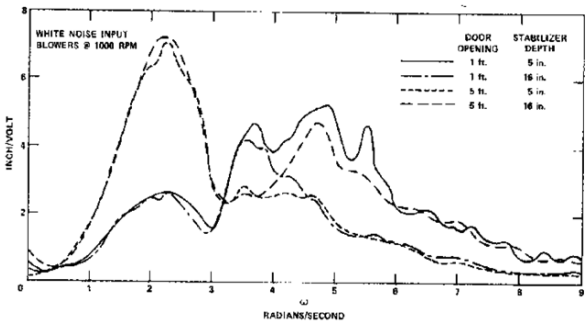

Figure 15. Example MASK Pneumatic Transfer Function.

Although a flap type wavemaker was first used by the Navy and then abandoned, the main advantage of that system is its linearity. The use of the EDL design that utilizes an air spring with its dryback design to reduce power required and using force as the major feedback created a superior alternative to the pneumatic.

The EDL designed directional wavemaker has 216 pivoting GRP paddles located along west and north sides of the MASK basin. The MASK is 98.3 m (322.5 ft) by 61.7 m (202.5 ft) in area and 6.1 m (20 ft) deep. The paddles have a pitch of 0.658 m (25.9 in), with a hinge depth of 2.5 m (8.2 ft) (Fig. 16).

This is a dry-back type wavemaker. It is driven by electric motors through a timing belt along a curved sector (Fig. 17). The hydrostatic force of the standing water on the wave paddle face is compensated for with air springs made from rubber bellows (Fig. 18). The waves are generated by an energy algorithm using paddle force as the primary feedback. A load cell at the top and bottom (Fig.18) measures the force used in the algorithm.

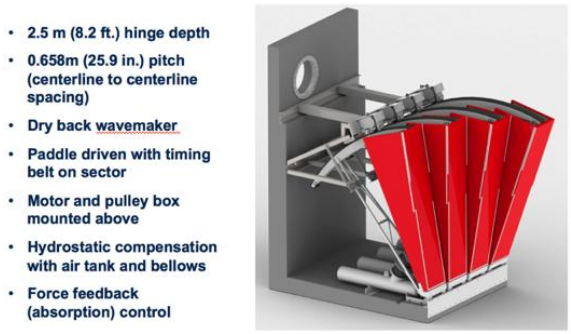

Figure 16. EDL Paddle Design.

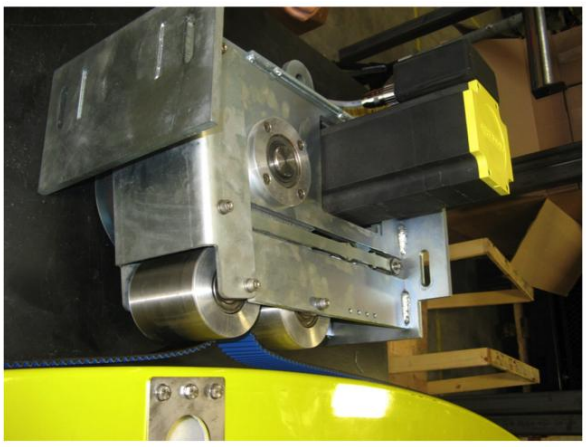

Figure 17. Pulley Box Drive Arrangement.

There are two additional design features of this wavemaker that have proven to improve the wave quality. A curved corner is used to minimize the singularity that is created with a square one as was used in the original pneumatic design. The control algorithm not only generates the commanded waveform, it also attempts to absorb any unwanted background wave energy such as beach reflections, model wake and most importantly the self-generated, second order cross-board waves.

The new wavemaker can produce multi-directional and short crested seas, multiple sea states at various headings, and synthesize wave grouping and episodic events. It is capable of producing regular waves having a 1/10 slope of 98 cm (38.6 in) in height. It can also produce a fully developed seaway (Pierson-Moskowitz spectral distribution) of 35 cm (14.6 in) in significant wave height and high steepness focused waves of 50 cm (19.7 in) in significant height (Fig. 19).

This wavemaker is capable of producing regular waves at oblique angles to the wave banks as well as both long crested and short crested irregular scaled seas. Using the directional capability, deterministic and focused wave events can be simulated.

Figure 18. Bellows and Lower Force Transducer

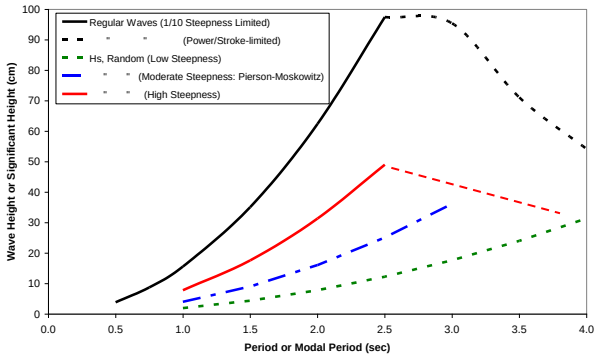

Figure 19. Wave Height Capability

Most any sea spectra can be produced, i.e., Pierson-Moskowitz, Bretschneider, JONSWAP and their varients are available. Other spectral forms and specific time histories can be easily added to the existing library using the Wave Generation software.

Another powerful capability of the new system is the ability to preview the commanded waves in 3D virtual space on the computer screen (Fig. 20). In this way, the test engineer can, prior to running the wavemaker, view the model sea. This allows the tester to make decisions relative to the placement of the model, course and direction, in order to maximize the interaction with the modeled seaway.

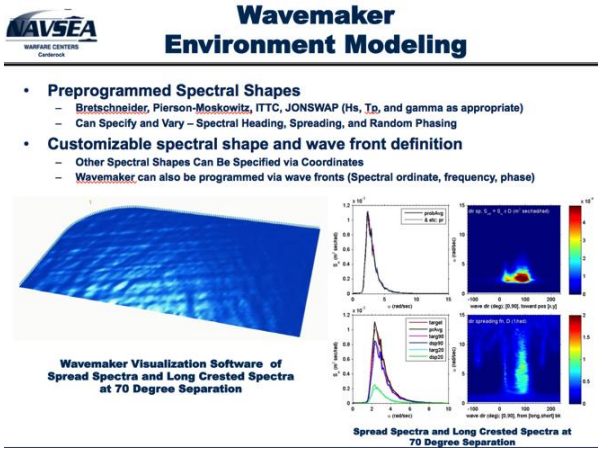

Figure 20. Virtual Wavemaker

4. Construction

The new MASK wavemaker was a sizeable construction project. During this six-year upgrade, MAR, Inc., was the prime contractor, with Edinburgh Designs Ltd., providing the design; Atlantic Industrial Technologies fabricating the major components, and Intelligent Controls and Power Reliability Systems, INCON was the contractor providing demolition of the existing equipment and installation of the new wavemaker and McLaren Engineering provided the concrete structural design. The actual mechanics of removal, construction of the new infrastructure, installation of the machine, tuning and calibration went very well (Fig. 21).

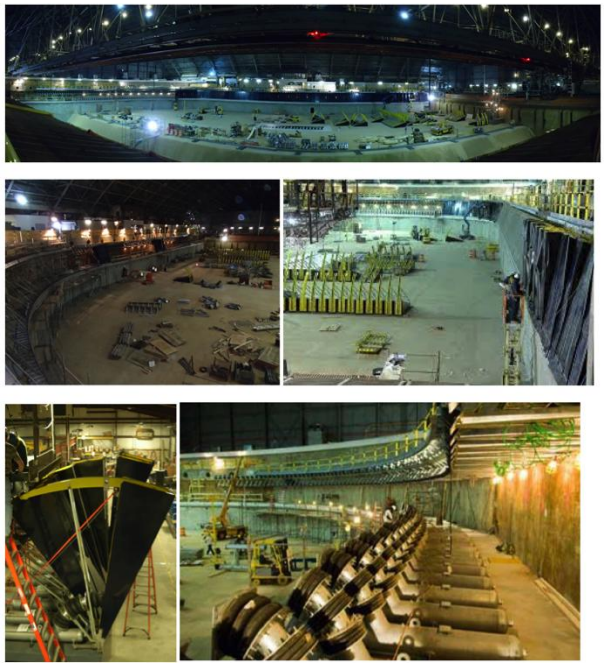

Figure 21. Construction.

"The Wavemaker Modernization team's biggest challenge was funding. The Team have led by example, working around difficult budget times, furloughs, and constantly adjusting work schedules in support of this critical Navy ship and ship systems testing facility upgrade, while maintaining the same high level of service to which their customers are accustomed," said CAPT. Richard Blank, commander, NSWC Carderock Division. "It's that sort of effort and dedication to NAVSEA and the NSWC Carderock team that allows our technical expertise to continually flourish for our Navy, for our nation." The end result is an advanced wavemaking facility, certainly the best processed by the United States Navy (Fig. 22).

Figure 22. New NSWCCD MASK Wavemaker

5. Using The New Machine

At present NSWCCD is in the learning stage: mastering the new capabilities and utilizing innovative test results to push the state-of-the-art in model sea generation and advancing the testing of advanced marine vehicles and ocean systems. A new Naval Combatant design has been evaluated in short crested seas for the first time. Following well planned and executed tests, technical papers will describe in detail both the capabilities and limitations of this new and valuable scientific resource.

Operation, from a manning perspective is little different than the old pneumatic wavemaker. One electrician operates the wavemaker, he is provided wave files by a test engineer, or directions during an iteration calibration, which now takes 2 to 3 iterations. An electrician or machinist is on call and performs periodic inspections while aiding in start up and shut down.

The single most noticeable feature of the new wavemaker is its sound, or lack of it. The old pneumatic wavemaker was very noisy. It was difficult to work in the area any length of time, and the noise generated by the generators and blowers penetrated the whole building and into the office spaces. Now, all that is heard are the breaking of the waves on the beaches.

The Naval Surface Warfare Center's David Taylor Model Basin performs work for Navy, DoD, Federal and State Governments as well as commercial entities. For more information regarding capabilities, scheduling, and availability, please contact:

Mr. Jon F. Etxegoien
jon.etxegoien@navy.mil
Head, Naval Architecture and Engineering Department, Naval Surface Warfare Center
Carderock Division

The Navy is always looking for talented and enthusiastic men and women. There are ongoing opportunities for students to obtain internship type employment. For more information on how to work with leading scientists or engineers at NSWCCD, please contact Recruitment at 1-877-441-1891 or visit Naval Sea Systems Command online at:

www.navsea.navy.mil/nswc/carderock/pub/career/student.aspx.

References

[1] Naval Surface Warfare Center, Carderock Division. Available online. URL: www.navsea.navy.mil/nswc/carderock/default.aspx. Accessed on December 19, 2014.

Session III Presentation

The Session III Presentation can be accessed online at URL:

http://scholarworks.uno.edu/oceanwaves/2015/Session3/

Session III Notes

Advances and issues in wave measurement technologies

These notes are intended as a supplement to the presentation "The Harold E. Saunders Maneuvering and Seakeeping (MASK) Facility New Directional Wavemaker." The following discussion points were captured by workshop rapporteurs:

- The new U.S. Navy paddle-driven wavemaker is much more effective than the former pneumatic wavemaker. The pneumatic wavemakers did not allow directional capabilities.
- Future capabilities with the paddle-driven wavemaker may support physical wave modeling in synchronization with waves measured from a wave buoy.
- *In-situ* wave measurements are sparse in the open ocean, but are useful for model verification or could be used in the analysis of satellite observations.
- Modeling efforts can be used to compensate for the inadequate number of *in-situ* wave measuring systems that are very unevenly distributed.
- Wave buoys come in a variety of shapes and sizes (i.e., spherical, discus, spar, or boat-shaped hulls). Algorithms use buoy response function to characterize wave motion.
- Organizations such as NOAA are involved in the calculation of measurement uncertainties, especially for different types of wave buoys. Assess differences in buoys with a main accelerometer sensor attached to a fine wire strain gauge in fluid on floating gimbal platform versus strapped down accelerometer.
- Use remote sensing imagery to extend observations from wave buoys and to support wave modeling.
- Innovations may support use of radar (coastal vs. deep ocean), improved measurement capabilities in marshes, and enhancements that allow modeling surf in wave tanks.
- Data telemetry is challenged in certain environments, for example in areas that are associated with sea ice. Development of the Hydrokite for air-sea interaction, data exfiltration, and challenging polar deployment sites has been initiated by Woods Hole Group. Hydrokite is a streamlined towed vehicle that is attached to a bottom mount or subsurface mooring.

- A program that considers tethered robotics would support wave modeling and ocean observations. Of interest would be the development of innovative data exfiltration technologies, especially during passage of tropical cyclones.

Session IV – Accessibility of wave information for scientists, engineers, and managers

Wave information is an important asset for safe and efficient marine operations. While it is difficult to put a value on accuracy and working standards, high quality information is a strategic asset. Those involved in ocean monitoring and the production of products require high quality data to characterize processes from micro to climatic scales. The following abstract and presentation describes the importance of using quality controlled wave information to support operators.

Extended Abstract

INTENTIONALLY BLANK

Establishing the Provenance of NDBC's Accuracy Statement for Directional Waves

Richard H. Bouchard [1)] and Rodney Riley[1)]
[1)] National Data Buoy Center (NDBC), Stennis Space Center, MS USA
[*]Corresponding author: richard.bouchard@noaa.gov

1. Introduction

The National Data Buoy Center (NDBC) has made measurements of wave directions from moored buoys for about 30 years. During that period, NDBC has fielded a variety of directional wave systems and has increased the number of stations with directional wave measurements as cost and size of the sensors and processing system have been reduced.

NDBC publishes an accuracy statement of 10° for wave directions

http://www.ndbc.noaa.gov/rsa.shtml.

However, the basis and traceability (or provenance) of that accuracy statement is not widely known or understood. Many of the analysis reports used to determine accuracy have not been published. NDBC is presently collecting and reviewing with the intent of publishing at least summaries of the methods used and the results.

This paper will review the basics of NDBC directional wave processing and terminology, and the common approaches NDBC has employed to make a determination of the accuracy of its wave direction measurements.

2. NDBC Directional Wave Parameters

NDBC uses the method of [1] for heave, pitch, and roll buoys to determine wave directions. The results of applying a Fast Fourier Transform are the first 5 Fourier Coefficients at each frequency. These Coefficients are then transformed into the four World Meteorological Organization [2] directional wave parameters at each frequency:

- Mean Wave Direction (α_1)
- Principal Wave Direction (α_2)
- First Normalized Polar Coordinate (r_1)
- Second Normalized Polar Coordinate (r_2)

The term *Mean Wave Direction* is also used as a short-hand for *Mean Wave Direction at the Peak Frequency* (MWD). *Peak Frequency* is the frequency of the most energy density in the spectrum. It is this latter use of the term *Mean Wave Direction* to which the accuracy statement generally refers. A complete description of NDBC's directional wave measurements can be found in [3].

3. Determination of Accuracy

The 10° accuracy claim can be traced to [4], although demonstrations of accuracy appear in the NDBC literature prior to this, and generally refer to the *Mean Wave Direction at the Peak Frequency.* The accuracy statement is one of the criteria used to certify or commission new wave systems for operational use. That determination is conducted by an intercomparison of a reference system, which is a previously certified or commissioned system, with a candidate system. The intercomparison is performed during a limited period field evaluation. The 10° metric is generally a *Root Mean Square Difference* (RMSD) and also generally confined to when the Peak Frequency is identical for both the reference and candidate systems.

4. Pre- and Post-deployment Directional Wave Calibrations

Recently NDBC undertook a program of bringing back buoys intact to conduct post-deployment calibrations of the buoy headings for comparison to their pre-deployment calibrations to determine the stability of the accuracy of the directional wave systems. This appears to be the first time such a comparison has been documented by NDBC. Pre-deployment calibrations require no more than a 4° error in buoy heading. Four systems, deployed for periods ranging from two to four years, were subjected to the same pre-deployment calibrations upon return to NDBC. Post-deployment errors of 6° to 8° indicate that there is no significant drift in wave directions for a normal deployment period.

5. References

[1] Longuet-Higgins, M.S, D.E. Cartwright, and N.D. Smith, Observations of the Directional Spectrum of Sea Waves Using the Motions of a Floating Buoy, *Ocean Wave Spectra*, Prentice Hall, Englewood Cliffs, NJ, pp. 111-136, 1963.
[2] World Meteorological Organization, FM 65-1 WAVEOB in *Manual on Codes, VI.1, Part A, WMO No. 306*, pp. A-129-132, 1995.
[3] National Data Buoy Center, *Nondirectional and Directional Wave Data Analysis Procedures, Technical Document 96-01*, 43 pp, 1996. Available online. URL: http://www.ndbc.noaa.gov/wavemeas.pdf.
[4] Gilhousen, D.B., NDBC Directional Wave Measurements, *Proceedings of Marine Instrumentation '90, San Diego, CA*

Session IV Presentation

The Session IV Presentation can be accessed online at URL:

http://scholarworks.uno.edu/oceanwaves/2015/Session4/

Session IV Notes

Accessibility off Wave Information or Scientists, Engineers, and Managers

These notes are intended as a supplement to the presentation, "Establishing the Provenance of NDBC's Accuracy Statement for Directional Waves." The following discussion points were captured by workshop rapporteurs:

- Some earlier archived National Data Buoy Center (NDBC) wave data do not accurately compare with more recent data.

- Wave measurement networks require reliable and effective instrumentation. Large 10-12m discus hull buoys are affected by currents that will confound wave measurements. NDBC limits distribution of directional data in real-time for frequencies below 0.20 Hz.

- Magnetometer-only wave sensors have been shown to have instances of inaccurate wave directions. These systems were primarly used in the Great Lakes and Gulf of Mexico, but are no longer in use by NDBC.

- Whenever possible, wind measurements should be made from the same platforms as the wave measurements.

- Geographical coverage of *in situ* data is limited owing to the expense of deployment and maintenance of wave buoys, but efforts are underway to reduce the size and cost and increase the reliability of buoy measurements. Geographic coverage can be limited by spatial correlations in which a limited number of *in situ* sensors can accurately characterize much larger areas.

- NOAA is involved in the assessment of quality from NDBC observations that cover past and present. The addition of new wave buoys is based on operational requirements.

- Operational organizations such as NDBC are testing and evaluating sensors on a pre-operational, operational, and post-operational basis.

- Data, analyses, and reports have not been standardized to account for the traditionally provided Mean Wave Direction Root Mean Square Deviation (RMSD), biases of the Mean Wave Direction, and statistics of the spreading factor 'r_1' (The First Normalized Component from the Fourier Coefficients).

- Define terms that facilitate the comparison of standard variables at a particular wave frequency (or period). For example, NDBC uses the terminology of the World Meteorological Organization (WMO) and the conventions of the International Association for Hydro-Environment Research and Engineering (IAHR). Similarly, at NDBC "Mean wave direction" really means mean wave direction at spectral peak.

- Differences exist in measured waves from different types of platforms, sensors, processing and moorings.

- Metadata is important to making data discoverable and useful to others. It is essential to properly account for observations from varying platforms, payloads and processing systems. Pre-2011 archives at the National Ocean Data Center (NODC) have limited metadata, but more than can be found presently on the NDBC website. Since 2011, increasing amounts of metadata are now included in the netCDF files.

- Wave measuring programs need to include available programmatic and technical publications, especially data reports. Publications should be developed that improve the confidence that users have for wave measurements coming from the various types of moored buoy systems, models, and fully-integrated solutions.

- Resources such as the Coastal and Ocean Modeling Testbed (COMT) facilitate evaluation of models and provides information on selected storms and input and output values for a variety of modeling systems.

Conclusions

This workshop has been designed to support those involved in producing maritime products that increase the efficiency and safety of marine operations. At a given seaport, a variety of professionals and skilled tradesmen benefit the global economy through interactions with ships that carry cargo into and out of seaports. Meteorological and oceanographic information, especially information on waves, supports those people who bring their products to market by sea and the people at the terminals who load and unload cargo. The findings from this workshop address improvements that are possible to cope with natural hazards such as changes in sea level, extreme waves, seiching, inundation, and methods. Of particular interest are hydrological risks and capabilities that facilitate the resumption of normal marine operations following severe weather such as hurricanes or tsunami.

Areas for improvement involve better characterization of the intensely non-linear transformations that take place in the shallow waters of the inner shelf and surf zone which play critical roles in driving the processes of coastal erosion, sediment redistribution and inundation height. Included among these processes are infragravity oscillations, wave set up and surf zone circulation (along-shore currents, rips etc.). Significant advances in recent years involving nearshore field experimentation and model development could benefit from activities that are facilitated by inter-comparisons and refinements. One example described during the workshop where this is being accomplished involves the Coastal and Ocean Modeling Testbed (COMT) which encour-

ages participation among various members of the marine technology community such as universities, government, and industry.

The Ocean Waves Workshop was initiated by applied oceanographers from Marine Information Resources Corporation and AXYS Technologies and basic researchers from the University of New Orleans to facilitate the transition of advanced buoy technologies, models, tools, toolkits and other capabilities to operational facilities and to improve the understanding and prediction of wave consequences for those involved in marine operations, naval architecture, ocean engineering, coastal construction, and product development. The Ocean Wave Workshop is held on odd years as a complement to the ONR/MTS Buoy Workshop which is held on even years.